University of California
Riverside

Fluid Inclusion Study of the Vein Mineralization in the VC-2A Corehole, Valles Caldera, New Mexico

A Thesis submitted in partial satisfaction
of the requirements for the degree of

Master of Science

in

Geological Sciences

by

Christine Marie Gonzalez

December, 1989

Thesis Committee:

Professor Michael A. McKibben, Chairperson

Professor Wilfred A. Elders

Dr. Alan E. Williams

The thesis of Christine Marie Gonzalez is approved:

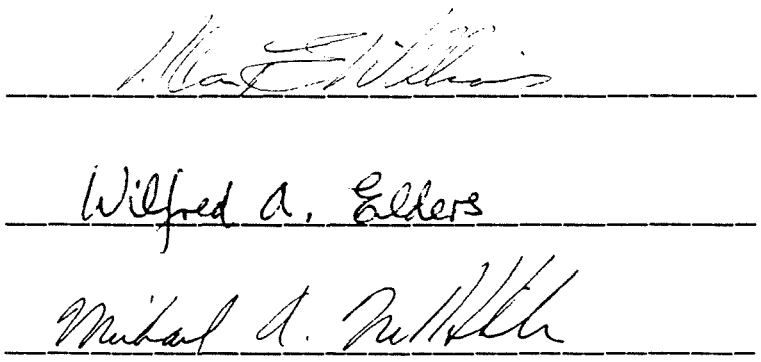

Committee Chairperson

University of California, Riverside

December, 1989

ACKNOWLEDGEMENTS

This study was made possible by funding from DOE Grant DE-FG03-85ER13408 to M. A. McKibben. I would like to thank Professor Mike McKibben for his encouragement and support, without which this work could not have been completed. I am grateful to my committee, Wilfred Elders and Al Williams, for their review and helpful discussions. I would especially like to thank Jeff Hulen of UURI for his review and contributions to this study and Chuck Herzig for his time and patience.

I would also like to acknowledge my parents, Dan and Betty Gonzalez, and my husband, David Headrick, for their daily patience and encouragement.

ABSTRACT OF THE THESIS

Fluid Inclusion Study of the Vein Mineralization

in the VC-2A Corehole, Valles Caldera, New Mexico

by

Christine Marie Gonzalez

Masters of Science, Graduate Program in Geological Sciences

University of California, Riverside, December 1989

Professor Michael A. McKibben, Chairperson

Valles caldera corehole VC-2A was drilled into the acid sulfate hot spring system of Sulphur Springs, New Mexico. The borehole was advanced 528 m through quartz-rich welded tuffs and volcaniclastic sandstones which contained secondary vein mineralization of quartz, pyrite, calcite, fluorite, molybdenite, and rhodocrosite. Although the system penetrated by VC-2A is now vapor-dominated, textures of the secondary mineralization

indicate that a liquid-dominated system was present at one time. It is thought that the system was boiling at the time of mineralization.

This study of fluid inclusions in vein minerals in the VC-2A core is designed to gain information on the conditions under which the mineralization occurred. Fluid inclusions from quartz and fluorite which occur between about 30 and 200 m depth, were generally liquid-dominated and had a salinity of <0.53 wt. % NaCl. Homogenization temperatures of primary inclusions in quartz were approximately 23°C higher than secondary inclusions, indicating that the system was cooling subsequent to quartz deposition. Homogenization temperatures of primary inclusions in quartz were also higher than those in fluorite by approximately 35°C. This suggests that the fluorite studied was deposited after the quartz. In order for these minerals to have been deposited at the temperatures revealed by homogenization, they had to have been at hydrostatic pressures corresponding to depths of approximately 200 m, as restricted by the boiling point curve. This depth is approximately 175 m greater than the present depth at which some of these minerals occur and has been accounted for in the literature by either erosion or a caldera lake.

One calcite sample from 522 m was studied. This sample was separated from the nearest quartz and fluorite studied by appoximately 300 m of tightly sealed rock. The fluid inclusions

in the calcite were liquid-dominated and had ice melting temperatures which indicated a salinity of 1.73 wt. % NaCl, somewhat greater than that of the quartz and fluorite inclusions. Homogenization temperatures of inclusions in the calcite were also higher. Primary inclusions were approximately 100°C higher and secondaries were about 50°C to 75°C higher than for the inclusions in the shallower quartz and fluorite samples. The higher temperatures and greater salinity may indicate that the calcite mineralized from fluids different than those higher in the section. Alternatively, it may be that as the fluids ascended, they were slightly cooled and diluted by meteoric water entering above the tightly sealed rock.

TABLE OF CONTENTS

TABLE OF CONTENTS, Continued

Page

LIST OF FIGURES

LIST OF FIGURES, continued

LIST OF FIGURES, continued

LIST OF PLATES

INTRODUCTION

The 528m deep Valles Caldera core hole 2A (VC-2A) was drilled into the Baca geothermal system of the Valles caldera at Sulphur Springs in New Mexico. Drilling was conducted under the Continental Scientific Drilling Program of the U. S. Department of Energy. The primary purpose of drilling was to penetrate an inferred vapor zone beneath the acid sulfate hot spring system of Sulphur Springs. Secondary objectives were to core through the interface between vapor and hot water-dominated zones, to obtain structural and stratigraphic information at the ring fracture-resurgent dome boundary, and to determine possible mechanisms of ore deposition in an active hydrothermal environment (Goff et al., 1987b).

The drilling revealed a shallow zone of sub-ore-grade molybdenum vein mineralization (Hulen et al., 1987). The present study was undertaken because analyzing fluid inclusions in vein material can provide valuable information about the temperature

and chemistry of the mineralizing fluid. This study of the fluid inclusions within secondary vein mineral phases is only part of many studies being undertaken in the hopes of better understanding the Valles caldera geothermal systems and their associated mineralization including the June 1988 drilling of VC-2B which is 30m northeast of VC-2A and1.8 km deep.

GEOLOGIC SETTING

The Valles caldera is located in north central New Mexico, 100 km north of Albuquerque. The caldera comprises a major portion of the central Jemez Mountains which are located at the intersection of the Jemez lineament and the Rio Grande rift (Figure1). Both linear tectonic features are presently active (Goff et al., 1981). The Jemez fault zone, which runs semiparallel to the trend of Canon de San Diego, is the surface expression of the Jemez lineament in the southwest Jemez Mountains (Goff et al., 1981). The Jemez lineament is made up of several volcanic fields which are Miocene to Quaternary in age. Most of the fields are composed of basalt but a few are of silicic lavas and tuffs. Of these fields, the Jemez Mountains volcanic field contains the largest volume of intermediate and silicic volcanics (Goff and Grigsby, 1982).

The Rio Grande rift is a continental rift which extends from Mexico into northern Colorado. Development of the rift began approximately 30 million years ago in the southern end and

Figure 1: Location of Jemez Mountains, New Mexico, showing the intersection of the Jemez lineament and the Rio Grande rift (Goff and Bolivar, 1982).

Figure 1

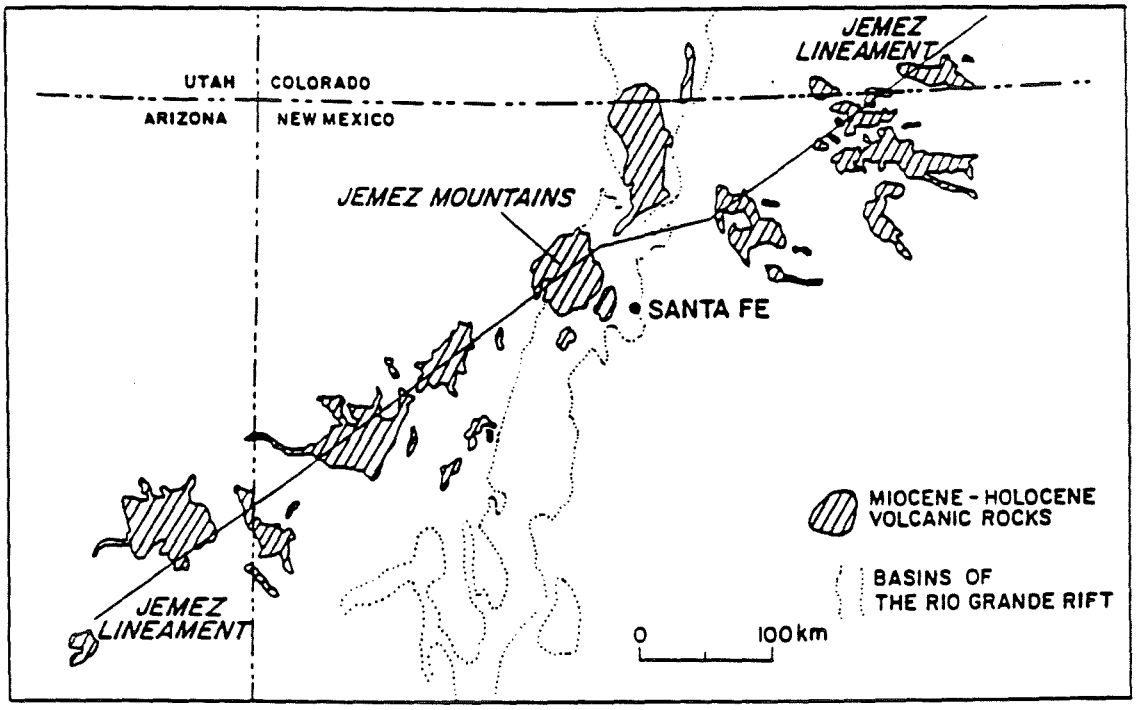
JEMEZ
LINEAMENT
UTAH
COLORADO
ARIZONA
NEW MEXICO
JEMEZ MOUNTAINS
SANTA FE
MIOCENE - HOLOCENE
VOLCANIC ROCKS
BASINS OF
THE RIO GRANDE RIFT
JEMEZ
LINEAMENT
0
100 km

progressed northward (Goff and Grigsby, 1982). In the Jemez Mountains region, the rift is composed of three en echelon segments, each filled with middle to late Tertiary sedimentary sequences (Goff and Grigsby, 1982).

The Valles caldera formed approximately 1.1 Ma b.p. near the end of a 10 Ma period of volcanic eruptions that formed the Jemez Mountains volcanic field (Goff et al., 1985c). Eruptions producing these volcanics began in late Miocene to early Pliocene with the extrusion of a basalt-rhyolite sequence followed by two complex basalt-andesite- dacite-rhyolite sequences (Smith and Bailey, 1968). Volcanism climaxed during the mid-Pleistocene with two or more eruptions of pyroclastic rhyolite ash deposited as the Bandelier Tuff. The first eruption produced the Toledo Caldera while the later ones produced the Valles caldera (Smith and Bailey, 1968). The Valles caldera floor collapsed several thousand meters during and after these eruptions, which produced ring fracture faults and truncated the southwest part of the Toledo caldera (Smith and Bailey, 1968; Goff and Grigsby,

1982). After collapse, the central floor was uplifted by resurgent doming and the moat area between the resurgent dome and the caldera walls was filled by rhyolite domes, flows, and tuffs (Figure 2) (Goff and Grigsby,1982).

Presently, the Valles caldera is a large subcircular depression with walls rising from a few tens of meters to more than 610m above the floor (Smith and Bailey, 1968). The caldera diameter ranges from 19km to 24km and the resurgent dome in the center has a base 13km to 16km in diameter. The dome peak has approximately 914m of relief with an average elevation of 3430m (Dondanville, 1978). The moat contains more than ten rhyolite domes which form a discontinuous ring of mountains, each ranging from less than 805m to greater than 3219m in diameter and having from 152m to 610m of relief (Smith and Bailey, 1968). The Bandelier Tuff within the caldera is 1829m thick, but is locally only over 305m thick outside the caldera due to simultaneous eruption and collapse of the Valles caldera (Dondanville, 1978).

Figure 2: Generalized geologic map of Jemez Mountains, New Mexico (Bailey and Smith, 1978).

Figure 2

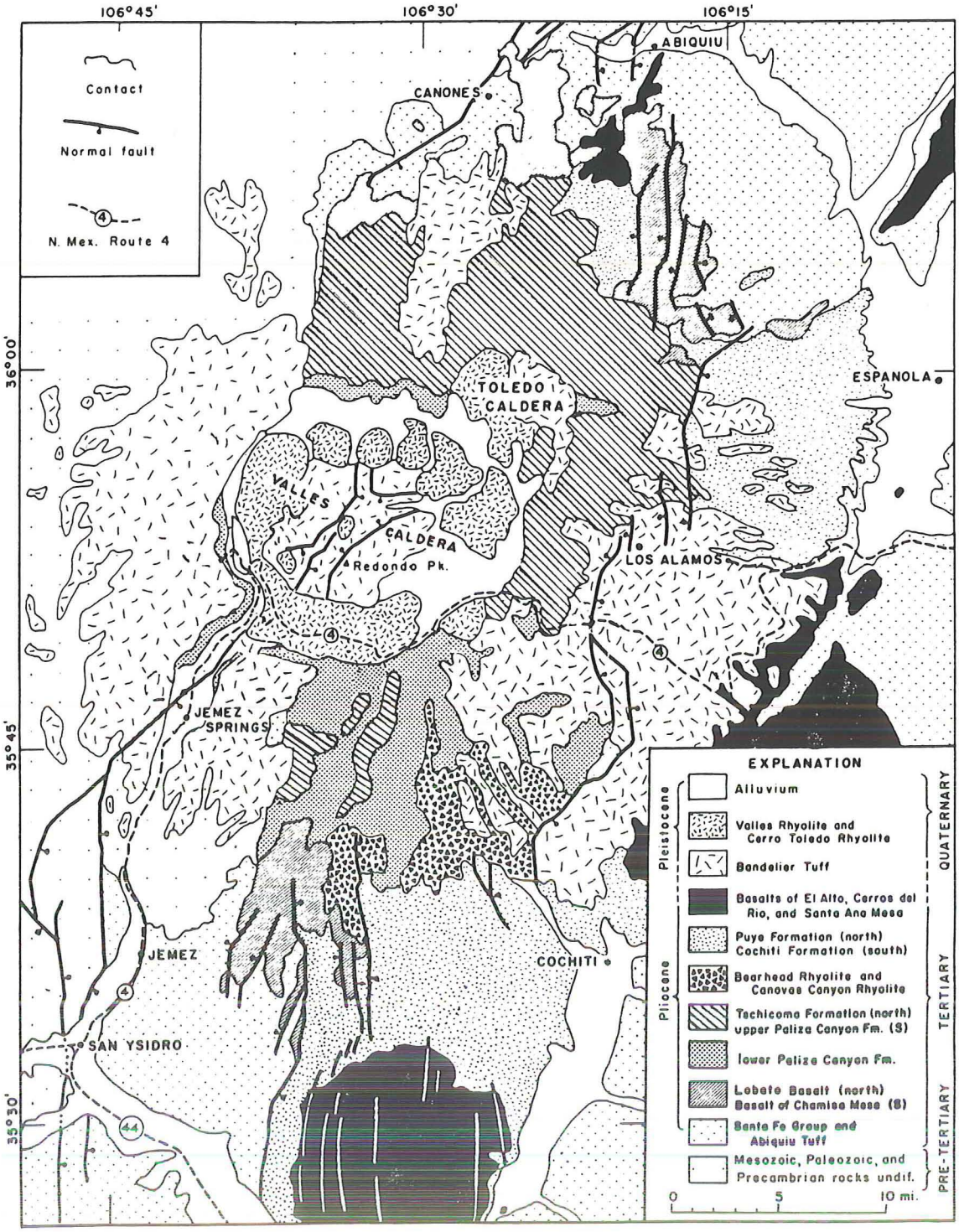
106°45'
106°30'
106°15'
36°00'
35°45'
35°30'
Contact
Normal fault
N. Mex. Route 4
ABIQUIU
CANONES
ESPANOLA
TOLEDO CALDERA
VALLES CALDERA
Redondo Pk.
LOS ALAMOS
JEMEZ SPRINGS
JEMEZ
COCHITI
SAN YSIDRO
EXPLANATION
Alluvium
Valles Rhyolite and Cerro Toledo Rhyolite
Bandelier Tuff
Basalts of El Alto, Cerros del Rio, and Santa Ana Mesa
Puye Formation (north) Cochiti Formation (south)
Bearhead Rhyolite and Canovas Canyon Rhyolite
Tschicoma Formation (north) upper Pelize Canyon Fm. (S)
lower Pelize Canyon Fm.
Lobato Basalt (north) Basalt of Chamisa Mesa (S)
Santa Fe Group and Abiquiu Tuff
Mesozoic, Paleozoic, and Precambrian rocks undif.
Pleistocene
Pliocene
QUATERNARY
TERTIARY
PRE-TERTIARY
0
5
10 mi.

The volcanics of the Valles caldera overlie relatively flat, undeformed, unmetamorphosed Paleozoic to Mesozoic marine carbonates, sandstones, shales, and evaporites of the Colorado Plateau (Goff et al., 1981; Goff and Grigsby, 1982). These sediments overlie Pre-Cambrian granite, gneiss, and schist. This entire sequence was progressively down-faulted into the Rio Grande rift towards the east during volcanism, resulting in volcanic sequences that progressively thicken eastward (Smith and Bailey, 1967; Goff and Grigsby, 1982).

Sulphur Springs is a well-studied region of hot spring and fumarole activity within the Valles caldera (Figure 3) on the west edge of the resurgent dome (Charles et al., 1968; Goff et al.,1985b). It is located in a 1.5 km wide graben-like structure which is bound by N and NE trending faults (Sulphur Creek, Short Canyon, and Freelove Canyon faults) (Figure 4). The hot springs lie at the intersection of the Sulphur Creek fault and three NW trending cross faults, the most important of which is the Bathhouse fault.

Figure 3: Valles caldera location map, showing VC-1, VC-2A, and VC-2B coreholes as well as Baca wells 4, 6, 7, 11, 12, 13, 15, 19, 20, and 24. The stippled area indicates surface hydrothermal alteration and the stars denote postcaldera rhyolite vents of the ring fracture system (Starquist, 1988).

Figure 3

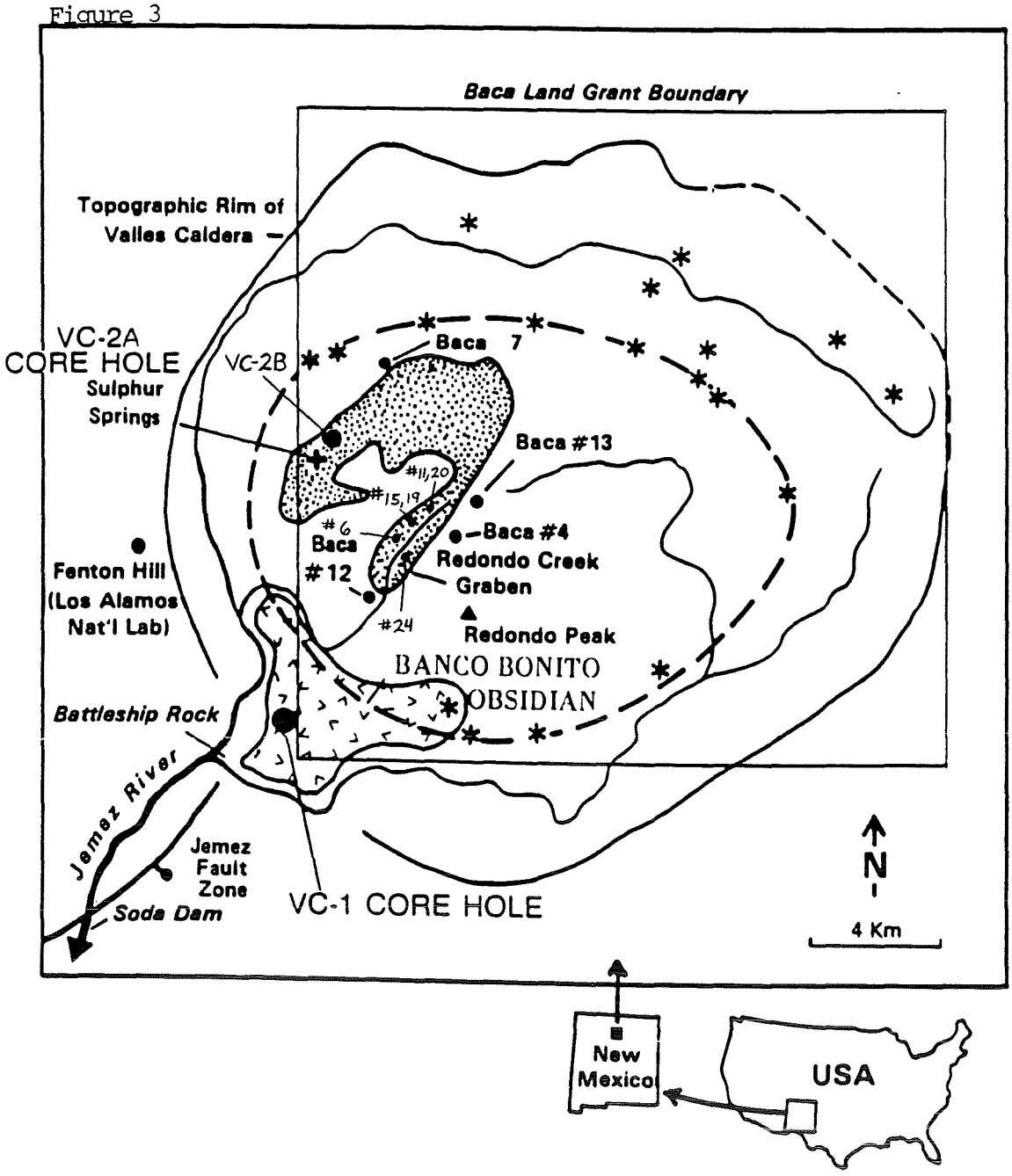
Baca Land Grant Boundary
Topographic Rim of Valles Caldera
VC-2A CORE HOLE
VC-2B
Sulphur Springs
Baca 7
Baca #13
#11,20
#15,19
#6
Baca #12
#24
Baca #4
Redondo Creek Graben
Redondo Peak
Fenton Hill (Los Alamos Nat'l Lab)
BANCO BONITO OBSIDIAN
Battleship Rock
Jemez River
Jemez Fault Zone
Soda Dam
VC-1 CORE HOLE
N
4 Km
New Mexico
USA

Figure 4: Sulphur Springs location map showing the positions of VC-2A and nearby geothermal wells, as well as the major faults (Charles et al., 1986).

Figure 4

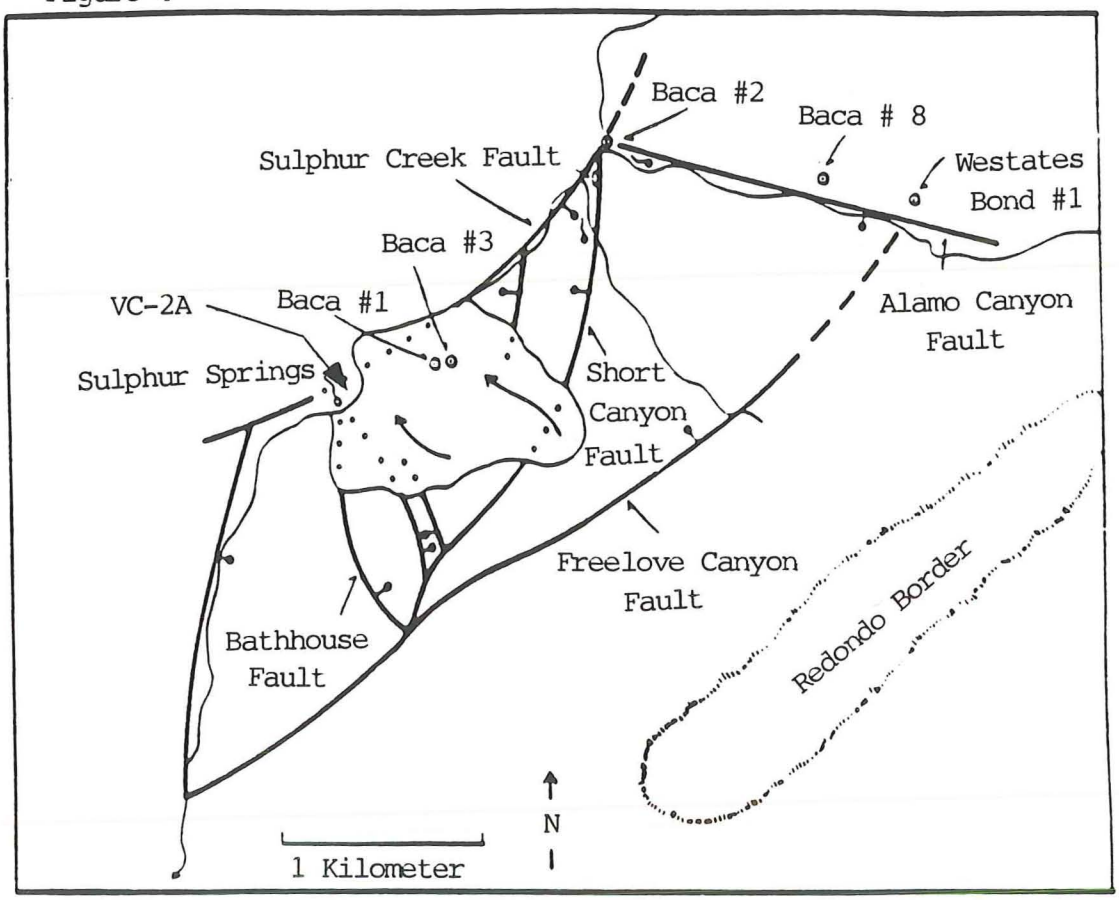
Baca #2
Baca # 8
Westates
Bond #1
Sulphur Creek Fault
Baca #3
VC-2A
Baca #1
Alamo Canyon
Fault
Sulphur Springs
Short
Canyon
Fault
Freelove Canyon
Fault
Redondo Border
Bathhouse
Fault
N
1 Kilometer

exhibit replacement of phenocrysts by microcrystalline adularia, albite, silica, and iron oxides. As alteration increases, montmorillonite appears in the host rock, which is subsequently cut by veinlets of alunite- kaolinite. Advanced argillic alteration occurs near active hot springs and fumaroles with the formation of kaolinite, alunogen ($Al_2(SO_4)_3 \cdot 17H_2O$), and halotichite (Goff et al., 1985b and Charles et al., 1986). Some of the rhyolites in this area have been leached to a porous, low density, siliceous residue while sulfur, gypsum, pyrite, ammonium sulfate, silica minerals and amorphous silica form next to the fumaroles and hot springs.

HYDROLOGY

Hydrothermal fluids of the Valles Caldera region have been described by Goff and Grigsby (1982) (see also Vuataz and Goff, 1986) and divided into three types: 1) Acid sulfate, 2) Thermal meteoric, and 3) Deep geothermal and derivative types. The first type is of particular interest because these waters are believed to be condensates of steam formed in vapor- dominated systems and are thought to be responsible for alteration near Sulphur Springs. The third fluid types are also of interest since boiling of them forms the vapor-dominated zone which in turn is the source of some components in the acid sulfate waters.

The deep geothermal waters occur in the keystone graben in a granophyrically recrystallized (Qtz + Kf + Ab), densely welded ignimbrite (Hulen 1988, personal communication) near Baca 4 (Figure 3) and contain approximately 7000 mg/kg total dissolved solids and significant concentrations of Na, Cl, and B as discussed by Goff and Grigsby (1982). Isotopically, the deep geothermal

fluids are enriched in ^{18}O resulting from high-temperature rock-water isotopic exchange. A distinctive ^{2}H component suggests that some connate fluids have possibly been derived from underlying paleozoic rocks. The derivative waters are found near Soda Dam and Jemez Springs and are isotopically intermediate between meteoric and deep geothermal fluids. They have ratios of Na, Cl, and B identical to the deep geothermal fluids. Goff and Grigsby (1982) explain the derivative types as resulting from leakage of the deep fluids laterally out of the caldera along the Jemez fault zone and mixing with surface water before discharging.

Three other hypotheses have been proposed since Goff and Grigsby's model. Truesdell and Janik (1986) described the deep geothermal fluids as isotopically heavy, low in radiogenic gases (^{4}He, ^{40}Ar), CO_2 and HCO_3, high in Ca, with a chlorinity near 2500 mg/kg and temperature of 260°C to 280°C. The derivative waters are described as isotopically light, high in radiogenic gases (^{4}He,

^{40}Ar), CO_2, and HCO_3, low in Ca, with a chlorinity near 1900 mg/kg and temperature of 290°C to 295°C.

Truesdell and Janik account for the variations in salinity and isotopic composition of deep geothermal and derivative types by dilution of a high-temperature, high salinity parent water (335°C and 2500 mg/kg Cl) to form the derivative waters and conductive cooling from the same parent to form the deep geothermal fluids (Baca wells 15, 24) with subsequent minor boiling in some cases (Baca well 19). The differences in Ca, HCO_3, CO_2, and He contents result from different leaching histories of the two fluids with little or no subsequent mixing of the hot waters. More specifically, the derivative fluids resulted from rapid upward flow through the Bandelier Tuff reservoir rocks after a long residence in pre-Bandelier sediments and Precambrian basement rocks and a 25% dilution with high-altitude cold groundwater from Redondo Peak. The deep geothermal fluids resulted from moving slowly through the Bandelier Tuff and cooling conductively. The short

residence of the deep geothermal fluids in the basement rocks left them low in radiogenic gases while the conductive cooling without mixing kept the original chloride and relatively heavy isotopic composition of the deep water.

White et al. (1984) and White (1986) propose that the differences between the two fluids resulted from adiabatic cooling during boiling and convective ascent of the derivative fluid (Baca wells 4, 6, 13) along the fault system in the reservoir. This was followed by conductive reheating during descent to produce the isotopically heavy deep geothermal fluids (Baca wells 11, 15, 19, 20). In this model, the derivative fluids are the parental fluids.

Smith and Kennedy (1985) explained the differences in fluid types by invoking mixing between a fluid containing radiogenic gases and mantle-derived helium (derivative fluids) and a second fluid with lighter gases that were isotopically encriched and resemble fractionated air (deep geothermal fluids). The gases in the derivative fluids were thought to represent magmatic gases while those in the deep geothermal fluids could have been leached

out of the Bandelier Tuff. These models are still being debated.

Thermal meteoric waters are found in the moat region of the caldera. These fluids are chemically dilute, of near-neutral pH, enriched in Li and B, and isotopically meteoric. They are simply composed of heated, near-surface groundwater.

The acid-sulfate waters, which discharge from faults and fractures within the resurgent dome, have a high SO_4 concentration (SO_4 = 2110 mg/kg), a low Cl concentration (Cl = 3.72 mg/kg), and a low pH. CO_2 is the dominant noncondensable gas and is most likely derived from thermal metamorphism of the Madera limestone which lies below the reservoir (Goff et al., 1985b). Oxygen isotopic data indicate that the water from the flowing acid spring is a steam condensate which is meteoric in origin, resembling the derivative waters. Water of a nearby bubbling mud pot is shifted towards an enriched value of ^{18}O having evolved through interaction with the hot host rocks and resembling the deep geothermal waters. However, the bubbling

mud pot fluids differ from the deep geothermal waters at least in containing far more SO_4 and far less Cl (personal communication, Hulen, 1988).

RESULTS OF COREHOLE VC-1

The Valles caldera corehole 1 (VC-1) was the first CSDP corehole drilled in the Valles caldera. Located near the intersection of the ring fracture zone and the pre-caldera Jemez fault zone (Figure 3), the corehole penetrated 298 m of intracaldera volcanics, 35 m of Tertiary volcaniclastic breccia that predates caldera formation, 91 m of Permian Abo formation, 381 m Pennsylvanian Madera limestone, and 40 m of Pennsylvanian Sandia formation (Figure 5) (Goff et al., 1985c and Goff et al., 1986). Molybdenite was identified in a fracture zone at 847 m. Thermal aquifers were penetrated at various intervals from about 510 m on down. Hydrothermal alteration is concentrated in sheared, brecciated, and fractured zones that occur from the volcaniclastic breccia to total depth (856 m), with both intensity and rank of alteration increasing with depth (Goff et al., 1985c). A major thermal aquifer produced fluids at approximately 90°C at 483 m. Chemically, the fluid resembled the high-temperature

Figure 5: VC-1 stratigraphy (Sasada, 1988).

Figure 5 VC-1 STRATIGRAPHY

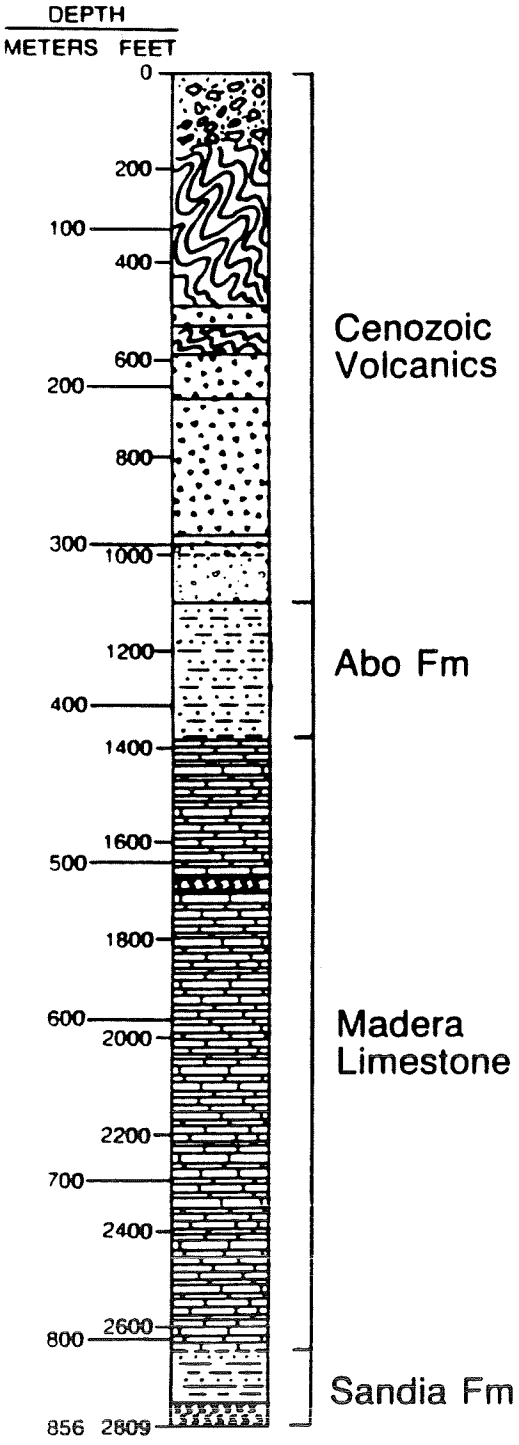

neutral-chloride fluids similar to those produced from other wells inside the Valles caldera and hot springs southwest of the caldera. This indicated that at least one aquifer of the deep geothermal/derivative fluid was intersected.

Although the bottom hole temperature (24 hours after completion) was 160°C, the present thermal regime is not hot enough to account for all secondary phases observed (chlorite, phengite, pyrite, and molybdenite). This fact, coupled with cross-cutting relations in veins and fractures, indicates that multiple hydrothermal events have affected the Paleozoic section in VC-1 for at least 1.1 My (Goff et al., 1985a).

COREHOLE VC-2A

The VC-2A corehole is located on the western edge of the resurgent dome in the western ring fracture zone of the Valles caldera at Sulphur Springs (Figure 3). Sulphur Springs was chosen as the location for VC-2A because it has the most intense fumarolic activity within the Valles caldera and because geochemical evidence indicates that a small vapor-dominated zone may exist below the area (Goff et al., 1985b). Prior to drilling, a boiling water table was estimated to be present at approximately 550 to 600 meters below the surface. Because the purpose of the well was to collect rock samples and allow for logging and testing in the vapor zone, drilling was planned to stop above the inferred water table (Nielson and Goff, 1985).

Drilling began on September 5, 1986 and lasted 24 days. A depth of 527.6 m was reached with 98% core recovery. The unequilibrated bottom hole temperature was 212°C as of November 1, 1986. Sub-ore grade molybdenite mineralization

was concentrated between 25 m and 125 m (Goff et al., 1987b; Hulen et al., 1987). The core is mainly composed of quartz-rich welded tuffs with a few volcaniclastic sandstones (Figure 6). The core is dissected by many veins completely or partially filled with secondary mineral phases. To a depth of approximately 150 m, quartz, pyrite, mixed layer illite/smectite, and illite are the main secondary phases. Minor phases include molybdenite and fluorite, with rhodochrosite, chalcopyrite, and sphalerite in trace amounts. Below 150 m the rocks contain scattered illite, chlorite, calcite, quartz, pyrite, and fluorite as secondary minerals. All of the rocks encountered have undergone moderate to intense hydrothermal alteration (Goff et al., 1987b).

Figure 6: VC-2A stratigraphy (Goff et al., 1987b).

Figure 6 VC-2A STRATIGRAPHY

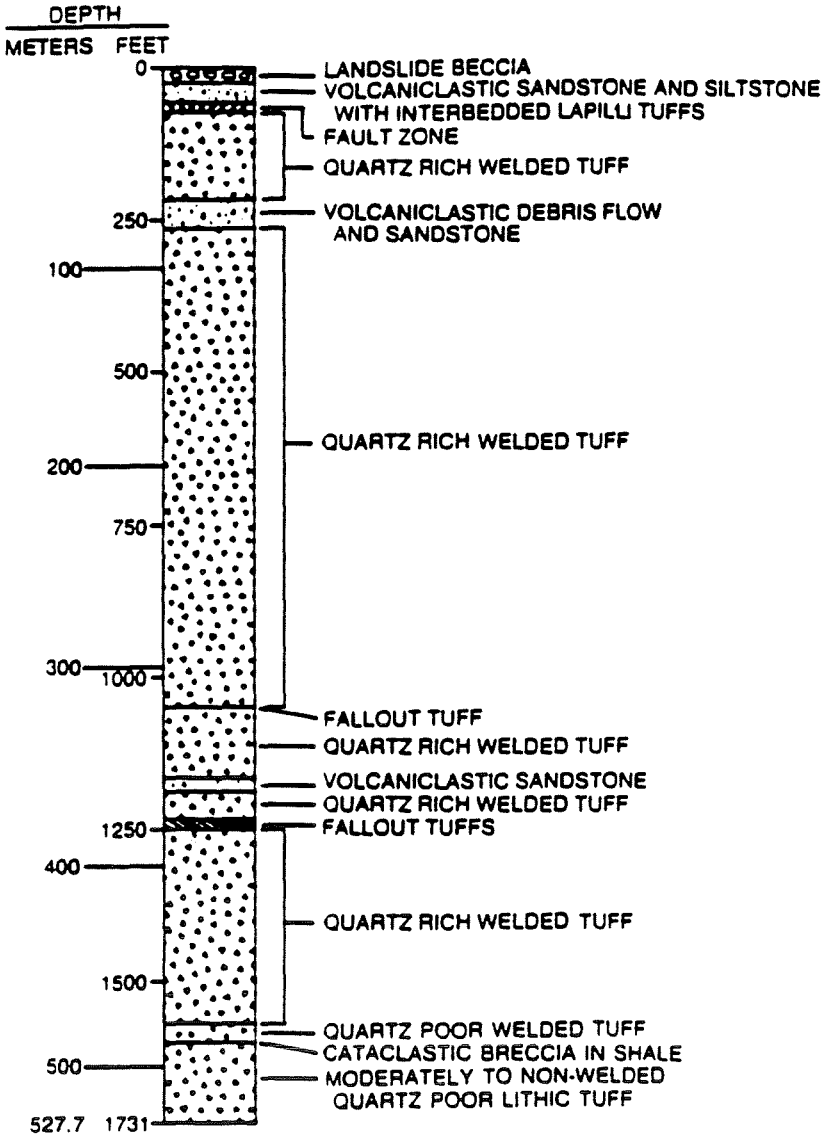

PREVIOUS WORK ON VC-2A

Preliminary results of studies by Goff et al. (1987b) indicated that the Sulphur Springs geothermal system is not a "true" vapor- dominated system containing dry steam. Instead, there is a surface acid sulfate condensation zone (< 5 m thick) lying above a subsurface boiling liquid- dominated reservoir. The vapor-rich zone extends down to at least 170 m and is separated from the hot water-dominated zone by a region of tightly sealed rock (Goff et al., 1987a). In the vapor-rich zone, the temperatures (approximately 212°C) and pressures (.414 MPa at 50 m - 100 m) are much lower than those in "true" (dry steam) vapor-dominated systems (236°C and 3.2 MPa). Goff et al. also note the occurrence of euhedral quartz crystals and an illite-quartz-molybdenite-fluorite vein assemblage at a depth of 30m in the borehole, indicating that the system was previously entirely water- dominated at a temperature of approximately 200°C. Since pure water under hydrostatic pressure at 200°C will be liquid

only at depths below approximately 200 m then a liquid phase must have extended above the present ground surface. Therefore, in order to explain the mineral assemblages observed at shallow depth, Goff et al. (1987b) suggest that host rocks to this liquid must have extended at least 175 m above the present level and were eroded subsequent to molybdenite deposition. This is assuming the ore-depositing fluid was not overpressured. Another explanation, as presented by Hulen et al. (1988), is that the formerly elevated liquid zone was due to the presence of a now-drained caldera lake.

Other work by Hulen et al. (1987) shows that the molybdenum was deposited as poorly crystalline molybdenite in veinlets and as breccia cement from very dilute liquid solutions. They report that molybdenite was intimately intergrown with the quartz and fluorite and therefore probably deposited with them at temperatures of approximately 200°C, based on preliminary fluid inclusion data from vein quartz and fluorite. They reported homogenization temperatures of 196.6°C to 226.2°C for primary

inclusions in fluorite and 190.1°C to 203.5°C for primary inclusions in quartz. These temperatures are much lower than those commonly interpreted for MoS_2 stockwork deposits (Westra and Keith, 1981; White et al., 1981). Deposition of molybdenite by liquid-dominated fluids at 200°C indicates that the system was at one time a hot water-dominated system which extended at least as high as 25 m beneath the present surface. Based on thermodynamic calculations at these temperatures, the molybdenite should coexist stably with quartz, pyrite, illite, sphalerite, and rhodochrosite in a relatively restricted part of log fO_2 - pH space (pH = 6-7, fO_2 = -45 to -40) (Hulen et al., 1987).

Bayhurst and Janecky (1987) studied the alteration mineralogy and geochemistry of the entire section and defined three general zones of alteration and mineralization. The upper molybdenum mineralized zone is characterized by molybdenum-bearing veinlets in felsic tuffs altered to illite and quartz. The middle zone is strongly altered to illite, chlorite, calcite, and

fluorite assemblages, but plagioclase is absent. The lower, moderately altered, zone is characterized by chloritic alteration with associated illite, calcite, and fluorite, in which original igneous textures and minerals are preserved.

Thermodynamic calculations by Janecky et al. (1987), based on the geochemistry of the molybdenum bearing assemblage, the fluid inclusion data, and the fluid composition of a similar nearby well (WC 23-4), imply that the equilibrium constant at 200°C is 19.5 ± 0.5 for the MoS_2 - forming reaction:

$$Mo^{++} + 2H_2S + 0.5O_2 = MoS_2 + 2H^+ + H_2O.$$

CORE DESCRIPTIONS

Dr. Michael A. McKibben examined the VC-2A core at Los Alamos National Laboratory and selected 50 core samples for fluid inclusion analysis from depths of 29 m to 197.3 m, with one sample at 522 m. Core samples with vein crystallization of quartz, fluorite, and/or calcite were selected. Brief descriptions of the cores selected are given in Appendix A; complete descriptions of the VC-2A cores have been made by Starquist (1988). The cores selected for this study consisted of altered tuffaceous material containing open vugs and subvertical fractures partially filled with euhedral quartz and pyrite. Lesser amounts of calcite, molybdenite, fluorite, chalcopyrite, rhodochrosite, sphalerite, and chlorite were also present. Euhedral quartz occurred in nearly all the core samples and its fluid inclusions were used extensively in this study.

Fluid inclusions in fluorite and calcite were also studied. The fluorite occurred as small crystal masses within veins, and in

one sample, VC-2A 122-7, as large vein crystals within an extremely altered tuff. Much of the calcite was too altered and opaque to find suitable inclusions. The fluid inclusions studied in calcite were from the deepest sample (522 m) where calcite occurred as large vein crystals. Core samples between approximately 200 m and 522 m were tightly sealed with little or no vein mineralization. The absence of cross cutting veins in any of the samples, prevented determining the sequence of vein generation. Hence relative time constraints could not be placed on the crystals being studied. Therefore, differentiating between primary and secondary inclusions was used to infer changes in fluid characteristics through time.

METHODS

Euhedral quartz crystals were collected from open veins in 30 core samples from depths of 29 m to 197.3 m. Fluorite crystal fragments were collected from depths of 59 m, 136.4 m, 164.6 m, and 197.3 m. One calcite sample from 522 m was also studied. However, because of the amount of tightly sealed rock between the calcite and the other samples, it is possible that mineralization occurred from very different fluids under very different conditions and therefore the data from this sample must be considered separately from that of the quartz and fluorite. Quartz crystals were picked from the open veins using a metal probe and a small, moistened paint brush. The quartz crystals ranged in length from less than 1mm to 1cm and in diameter from 0.5 mm to 3 mm. However, most of those studied were of small diameter (0.5 mm to 1 mm) for optical purposes (eg., clarity, translucence). Fluorite cleavage fragments were picked out or carefully chipped off larger crystals. The calcite cleavage fragments were broken

off a large vein sample. After viewing all crystal and cleavage faces under the polarizing microscope to determine the optimum orientation for study, the samples were mounted on cover glasses (1 to 5 crystals per glass) with "Krazy Glue", a proprietary brand of cyanoacrylate adhesive. Calcite samples were polished for better viewing but quartz and fluorite samples did not require polishing. Locations and shapes of the fluid inclusions in each chip were then mapped out on paper and numbered so that information from different studies (i.e. freezing and heating runs) could be recorded for the same inclusion. Liquid to vapor volume ratios at room temperature were estimated and inclusion diameter (longest) and vapor bubble diameter were measured prior to freezing and heating.

Freezing and heating measurements were made using a Nikon Optiphot petrographic microscope equipped with an adapted U.S.G.S. gas- flow heating/freezing system purchased from Fluid, Inc. Freezing was conducted prior to heating since heating can cause inclusions to expand to the point where they

fracture the host mineral; this is especially true for calcite and fluorite. Approximately 540 inclusions were originally studied, many of which were identified later as necked inclusions which resulted in confusing preliminary results. The results presented in this study are based on 121 non-necked inclusions which resulted when the original 540 inclusions were re-examined for potential necking.

Identification of Inclusion Types

Criteria used to identify primary (formed during crystal growth) and secondary (formed after crystal growth) inclusions were taken from Roedder (1984). Inclusions were identified as primary when they were isolated away from other inclusions (Plate 1). Inclusions were identified as secondary when they occurred as planar groups aligned along healed fractures (Plate 2). Pseudosecondary inclusions are those that formed along fracture planes under the same fluid conditions as the primary inclusions. Although pseudosecondary inclusions resemble secondary

inclusions, they were identified by homogenization temperatures and liquid to vapor ratios which were similar to inclusions classified as primary. For this study, pseudosecondary inclusions were classified as primary.

Necking-down is a process of recrystallization resulting in the formation of several smaller inclusions that have the same total volume as the original single inclusion (Plate 3) (Roedder, 1984). Nearly all secondary inclusions are a result of necking down as a fracture heals. However, necked inclusions can cause erroneous homogenization temeratures if the necking occurred after a vapor bubble had formed, since the liquid-to-vapor ratio would no longer reflect the temperature at which the inclusion was trapped. Necked inclusions were identified as those which appeared to be related but had varying liquid to vapor ratios and liquid-rich inclusions surrounded by vapor-rich inclusions. Necked inclusions were not used in the analysis. Sometimes it is difficult to determine if an inclusion has necked if the process has just begun and has pinched off a portion which may still apppear

connected to the main inclusion. For this study, inclusions with long, thin protrusions which may not have been connected to the main body of the inclusion were not analyzed. Vapor-rich inclusions not resulting from necking were identified when such inclusions were separated from other inclusions and otherwise appeared to be primary (Plate 4). Such occurrences were found in two fluorite samples (59.0 m and 197.3 m) and in two quartz samples (29.0 m and 47.9 m). Only one (47.9 m), however, exhibited observable ice crystals growing and melting during melting temperature measurements and none exhibited observable phase changes during homogenization temperature measurements.

Crushing Methods

Crushing studies were conducted on samples that had not been heated or cooled by use of a M. K. Lantham Enterprises crusing stage with Type A immersion oil and alkaline $BaCl_2$ solution as mediums. Samples to be crushed were placed between

two glass slides in a drop of fluid medium. This was then set in the crushing stage which was placed on the microscope stage. The two slides were slowly pressed together by turning the screwing mechanism of the crusher until the crystal began fracturing. Squeezing the slides together continued while the crystal fractured and released trapped fluids into the medium. The immersion oil is used to determine if the gas pressure is above or below 1 atm (if the vapor bubble expands or contracts upon release, respectively). The alkaline $BaCl_2$ is used to determine if the gas is CO_2 by the precipitation of witherite. Also, CO_2 can be distinguished from CH_4 since CO_2 dissolves slowly in an immersion oil medium while CH_4 dissolves rapidly. The results are reversed when $BaCl_2$ is used as the medium.

Both quartz and fluorite samples were crushed, however, fluorite yielded better results because it crushed easily. Quartz was more difficult to crush and often the slides broke before the quartz crystal fractured.

RESULTS

The inclusions analyzed generally ranged from 6 to 18 micrometers in diameter, were liquid-rich, and homogenized to the liquid phase. A few vapor-rich inclusions were identified. Liquid to vapor volume ratios of the liquid-rich inclusions ranged from 85% to 95% liquid. Vapor-rich inclusions occurred together with liquid-rich inclusions in a few samples but homogenization of the vapor-rich inclusions was not detectable. Results of the fluid inclusion analysis are shown in Appendix B.

Eutectic Temperature

Due to the extremely low salinities of the fluid inclusions (see Ice Melting Temperature, below) the eutectic temperature was approximately equal to the melting temperature of the ice. This made the beginning of melting difficult to observe and so the eutectic temperature could not be accurately measured.

Ice Melting Temperature

The refractive indices of pure water and ice are nearly identical and so ice melting in these inclusions was difficult to observe. For this reason, the ice melting temperature (Tmi) was usually determined by watching the vapor bubble rapidly expand to full size while heating indicating that the ice was completely melted.

Ice melting temperatures of primary inclusions ranged narrowly from 0.0°C to -0.3°C (±0.1°C) in both quartz and fluorite samples (Figures 7A, 8A). Tmi of secondary inclusions in quartz and fluorite also ranged from 0.0°C to -0.3°C (Figures 7B, 8B). Tmi of a primary inclusion in the calcite sample was -0.5°C. Secondary inclusions in the calcite sample had ice melting temperatures which ranged from 0.0°C to -1.0°C (Figure 9A). Figures 7C and 7D show that the ice melting temperatures of primary and secondary inclusions in quartz do not vary systematically with depth. This appears to be true for inclusions in fluorite (Figures 8C, 8D), although more data would be necessary to be certain.

Figure 7A: Ice melting temperature of primary inclusions in quartz.

Figure 7B: Ice melting temperature of secondary inclusions in quartz.

Figure 7A

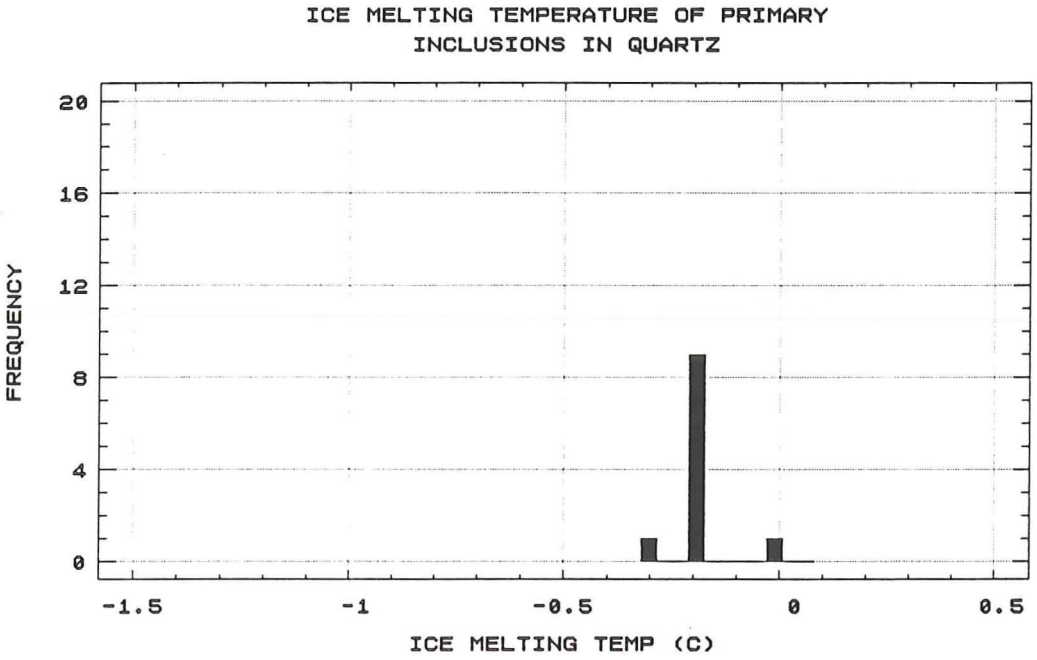

Figure 7B

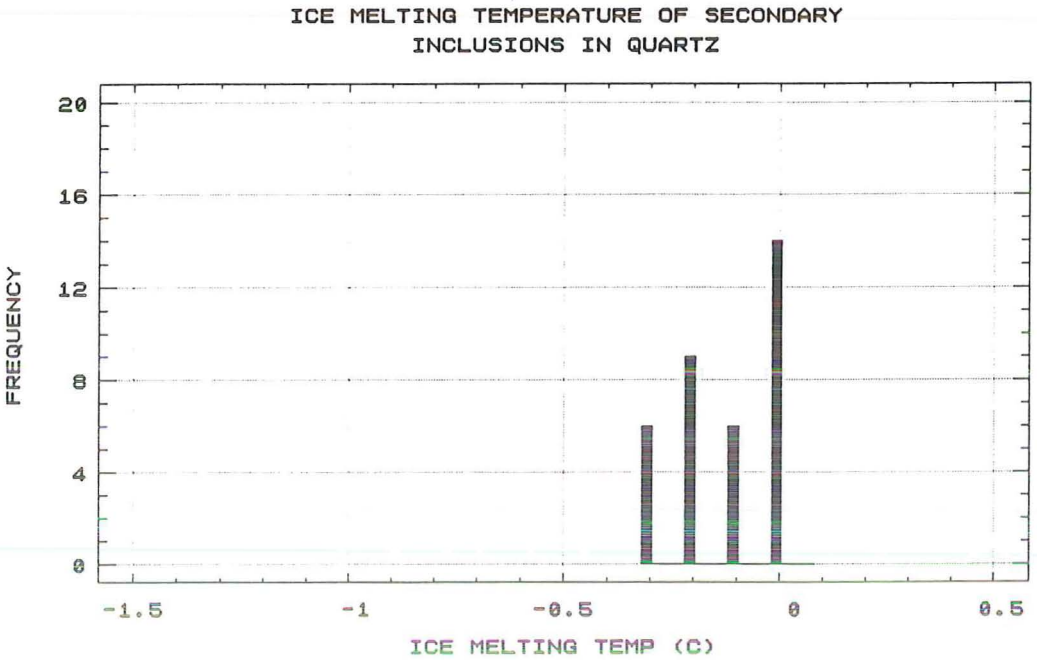

Figure 7C: Ice melting temperature vs. depth for primary inclusions in quartz.

Figure 7D: Ice melting temperature vs. depth for secondary inclusions in quartz.

Figure 7C

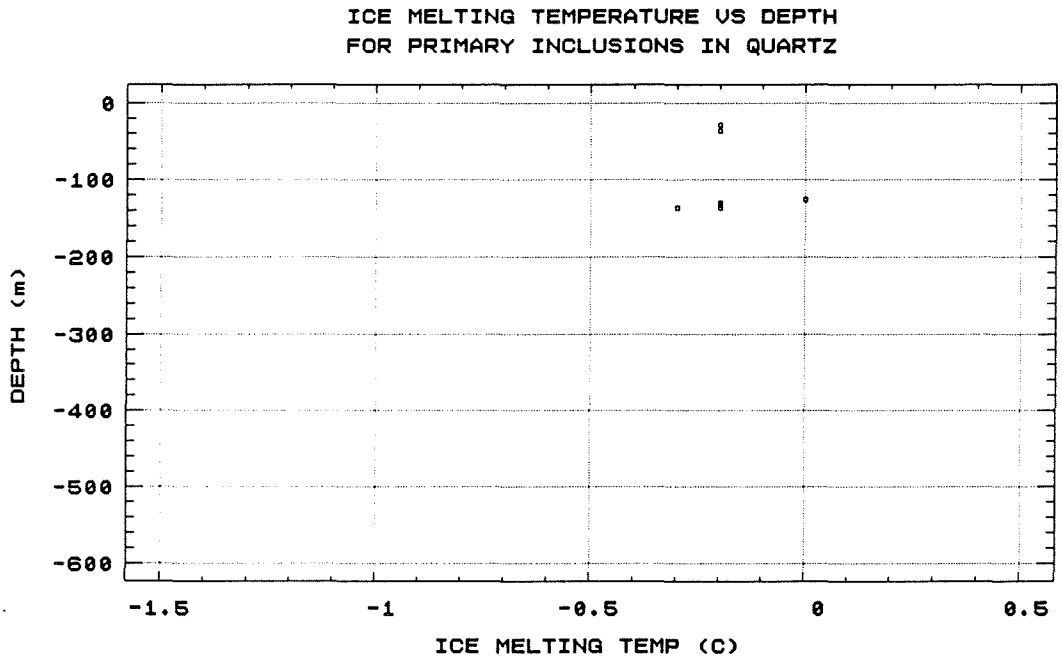

Figure 7D

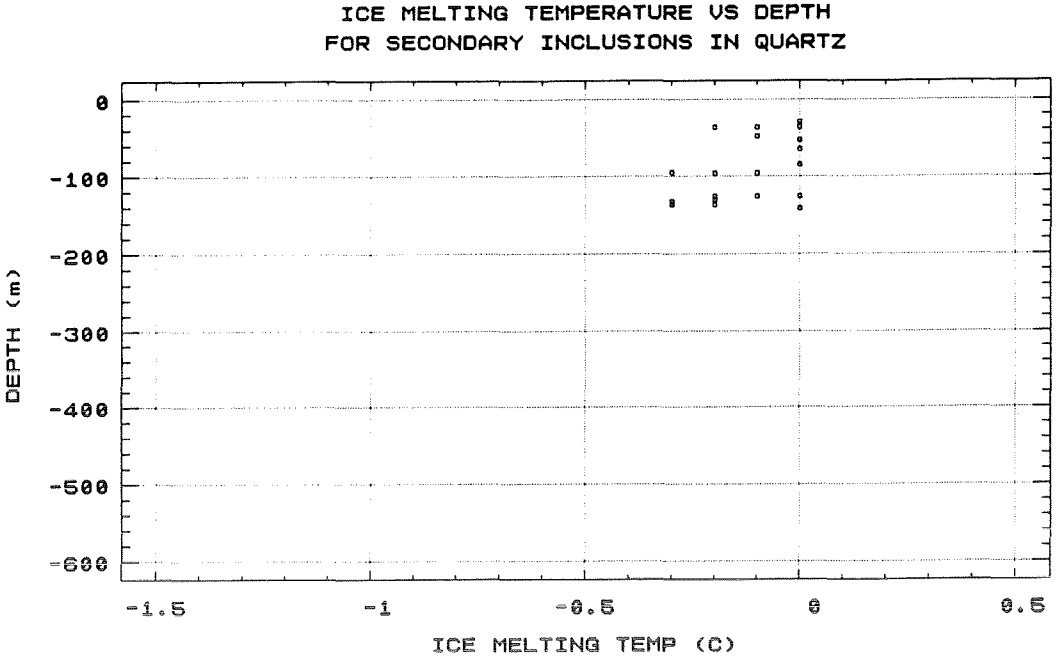

Figure 8A: Ice melting temperature of primary inclusions in fluorite.

Figure 8B: Ice melting temperature of secondary inclusions in fluorite.

Figure 8A

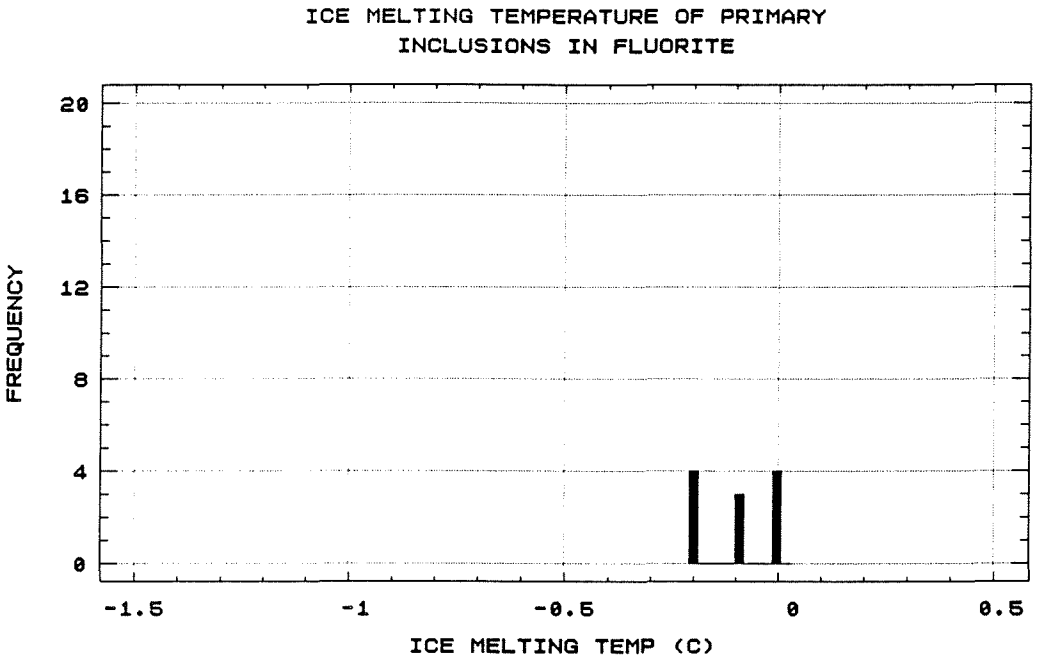

Figure 8B

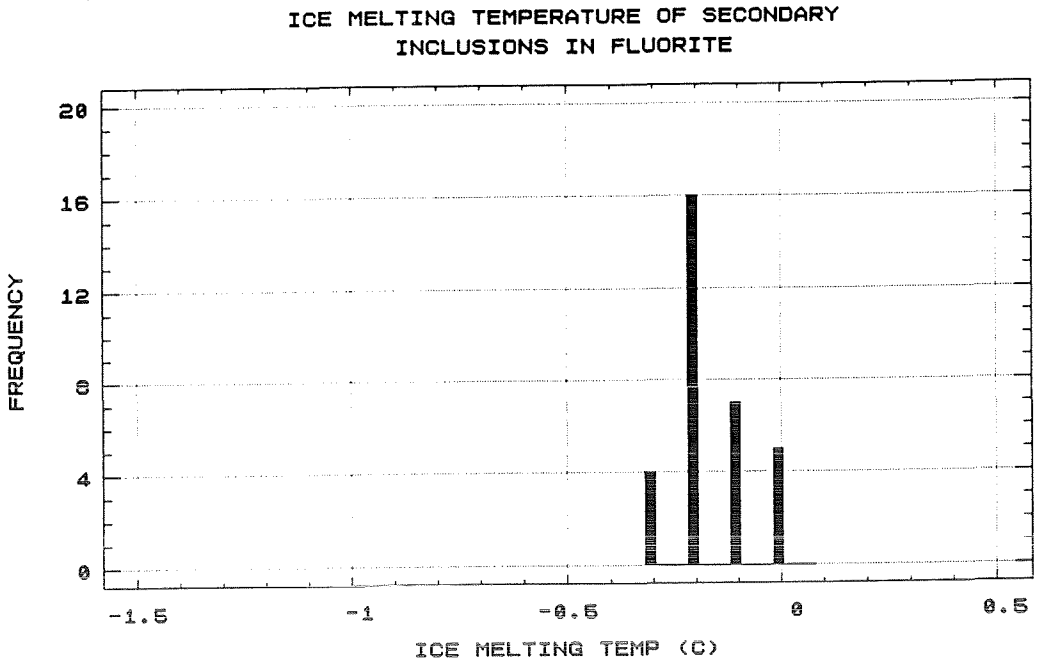

Figure 8C: Ice melting temperature vs. depth for primary inclusions in fluorite.

Figure 8D: Ice melting temperature vs. depth for secondary inclusions in fluorite.

Figure 8C

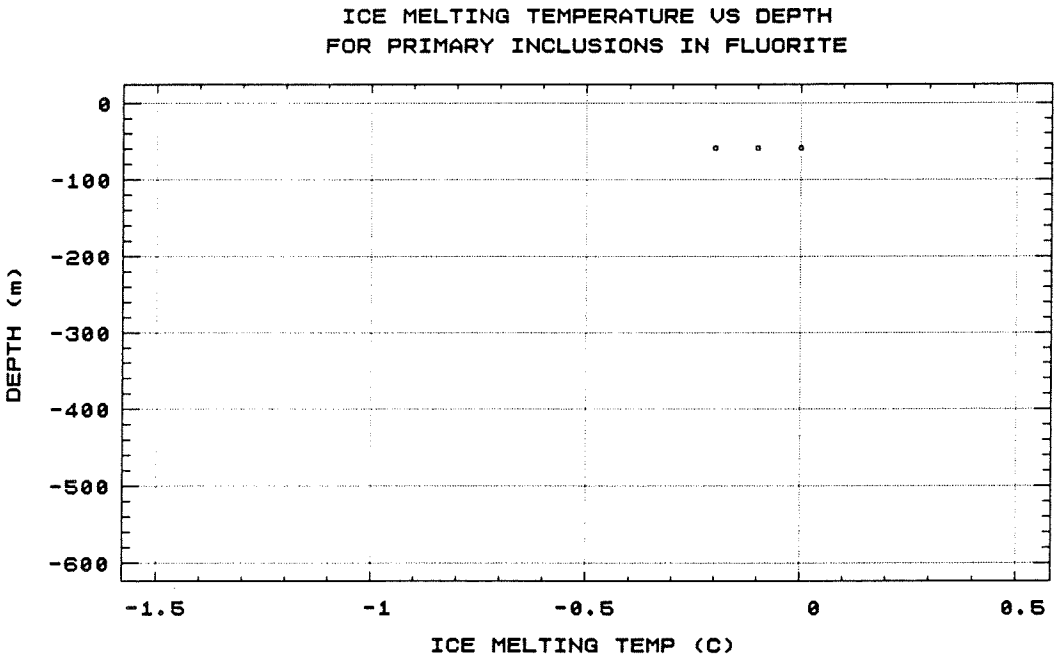

Figure 8D

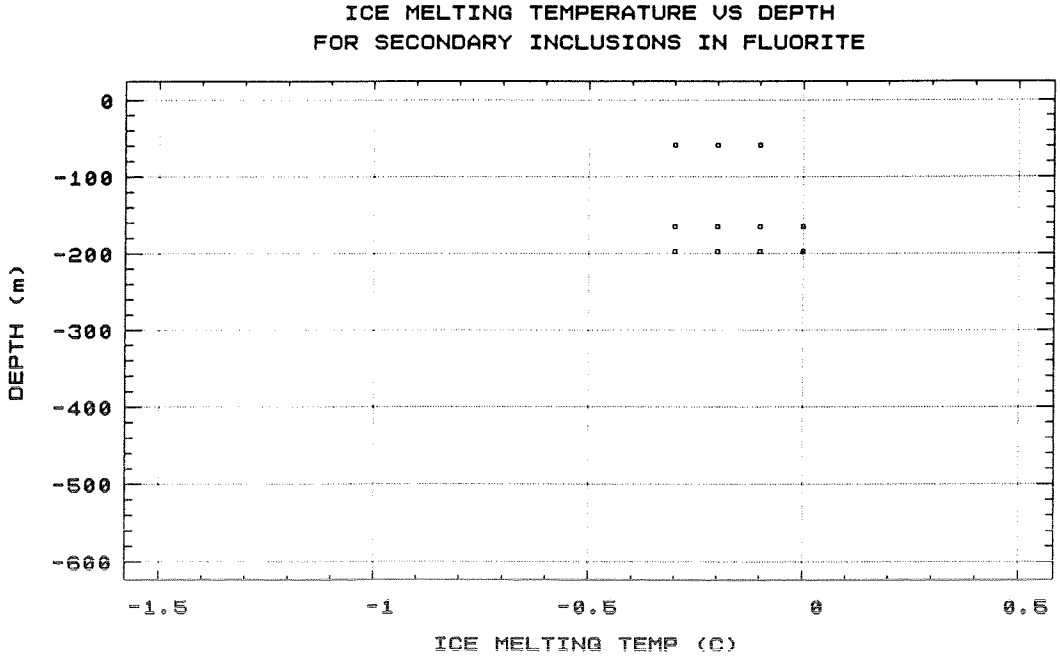

Figure 9A: Ice melting temperature of secondary inclusions in calcite.

Figure 9B: Homogenization temperature of secondary inclusions in calcite.

Figure 9A

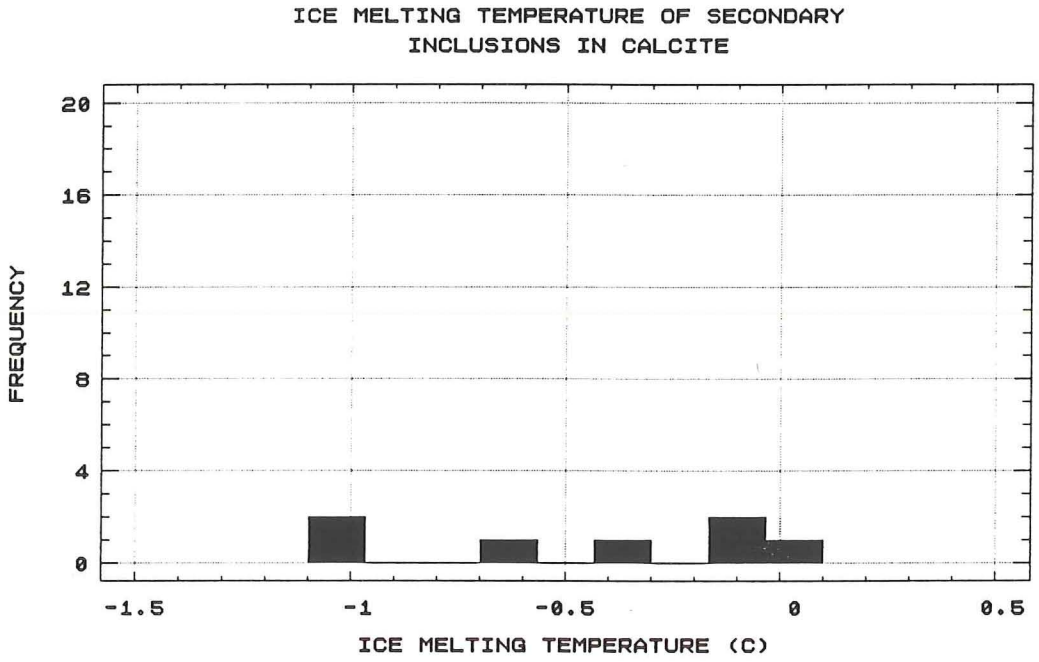

Figure 9B

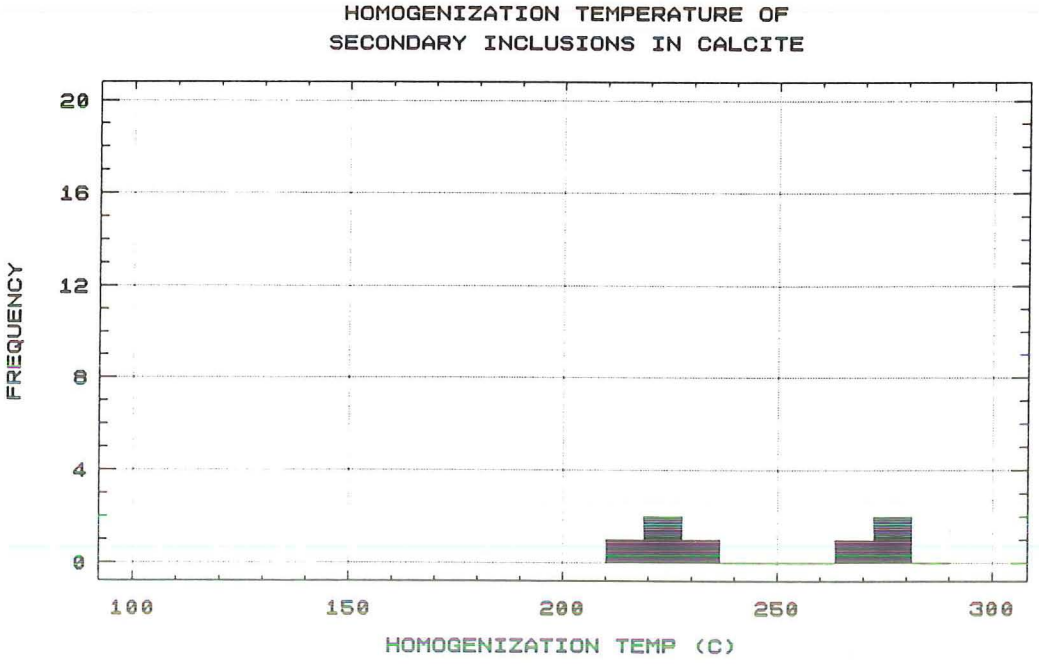

Homogenization Temperature

Quartz

The mean homogenization temperature (Th) of primary inclusions in quartz is approximately 213°C, with a range of 195°C to 240°C (Figure 10A). Most (± one standard deviation from the mean) occur between 201°C and 225°C. The few temperatures lying outside of this range may be erroneous due to necking. Secondary inclusions in quartz show a much greater range in homogenization temperature, 150°C to 225°C (Figure 10B) with a mean of approximately 190°C. Most (± one standard deviation from the mean) of the temperatures are less than 204°C and greater than 174°C. Temperatures at the high end of the range may be erroneous due to necking or may be pseudosecondary (in which case the temperatures would resemble those of primary inclusions). Temperatures at the low end may be erroneous due to necking. Figures 10C and 10D show that the homogenization temperature of both primary and secondary inclusions does not vary systematically with depth (bars represent homogenization

Figure 10A: Homogenization temperature of primary inclusions in quartz.

Figure 10B: Homogenization temperature of secondary inclusions in quartz.

Figure 10A

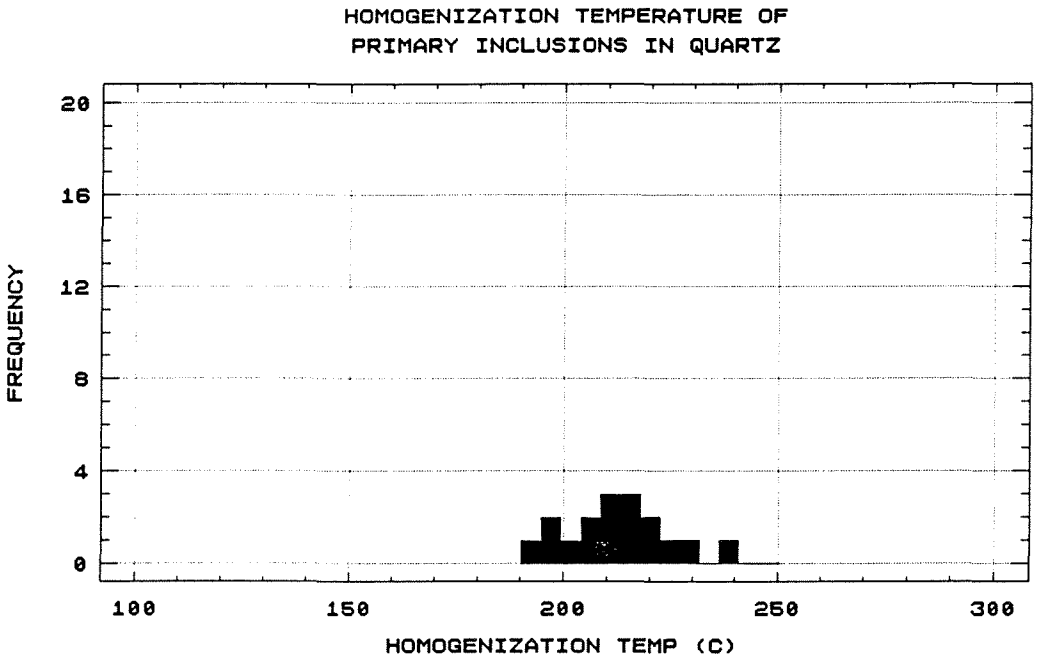

Figure 10B

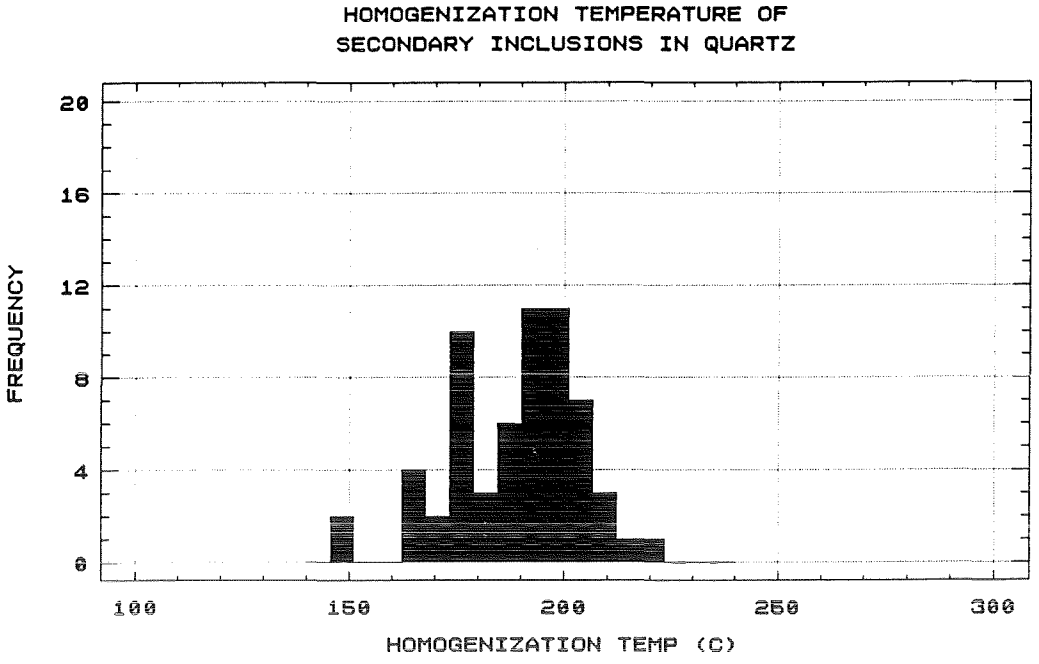

Figure 10C: Homogenization temperature vs. depth for primary inclusions in quartz.

Figure10D: Homogenization temperature vs. depth for secondary inclusions in quartz.

Figure 10C

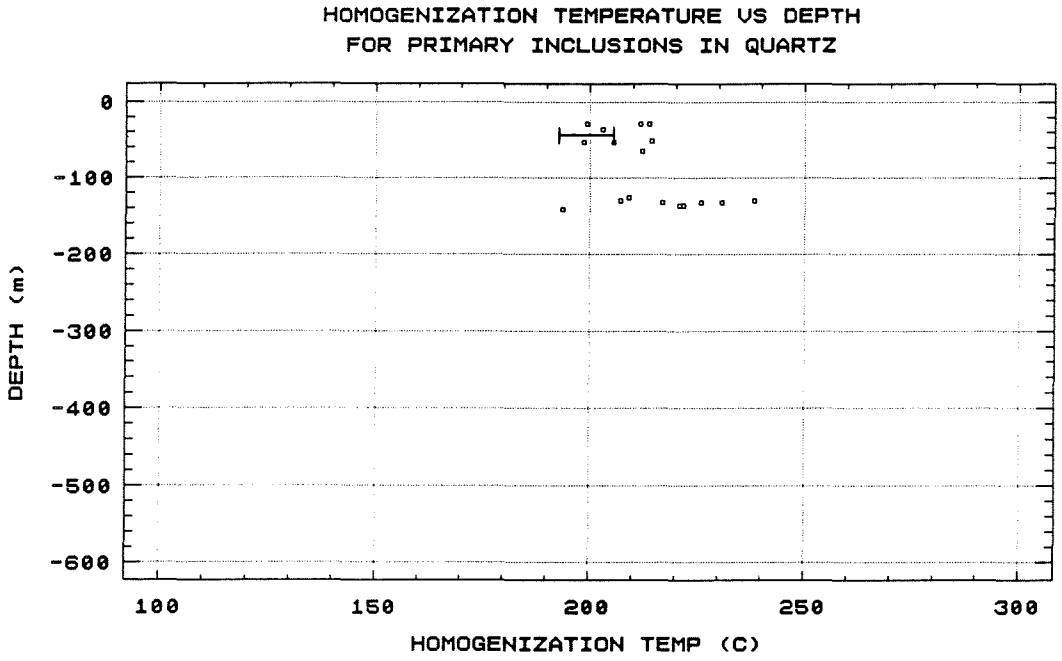

Figure 10D

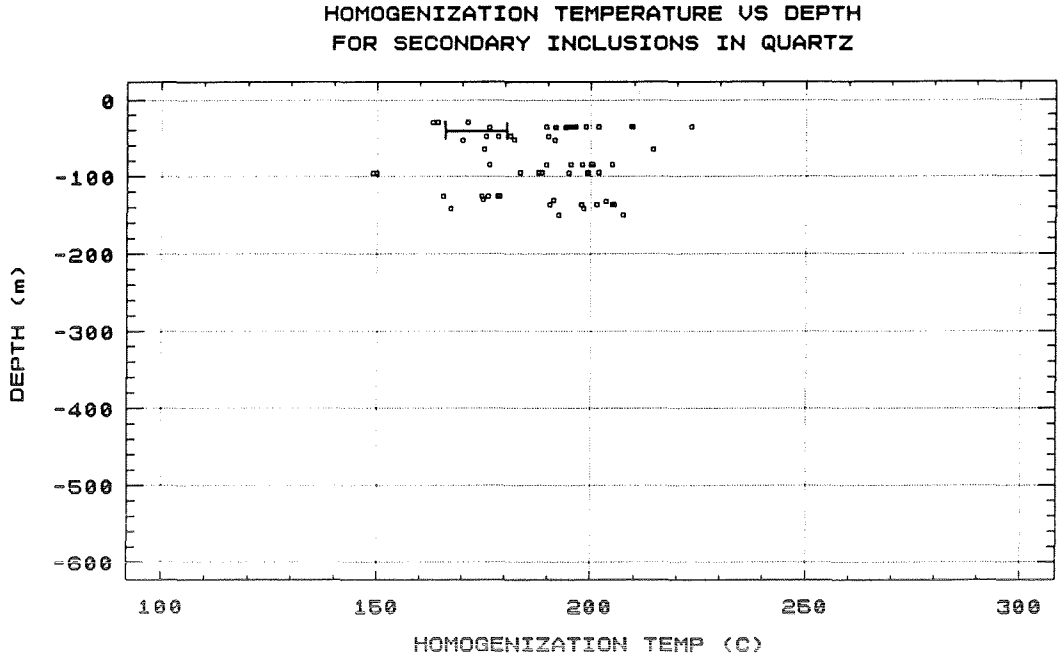

temperatures of inclusions in quartz presented by Hulen et al. (1987)). These temperatures are considerably greater than the unequilibrated downhole temperature log of the well measured in November of 1986 (Goff et al., 1987b) (Figure 11A, 11B). The downhole temperature log of April 1987 showed an increase of less than 5°C in downhole temperature over the November log (Musgrave et al., 1989). Figures 11A and 11B also illustrate that all primary inclusions but not all secondary inclusions in quartz homogenized at temperatures greater than the boiling point curve of pure water.

Fluorite

The homogenization temperatures of primary inclusions in fluorite range from 160°C to 200°C (Figures 12A, 12C). Bars shown on figure 12C represent homogenization temperatures of primary inclusions in fluorite presented by Hulen et al. (1987); data for secondary inclusions in fluorite were not given in that report. Homogenization temperatures of secondary inclusions in

Figure 11A: VC-2A downhole temperature log with Th of primary inclusions in quartz, together with the boiling curve for pure water (Haas, 1971).

Figure 11B: VC-2A downhole temperature log with Th of secondary inclusions in quartz.

Figure 11A

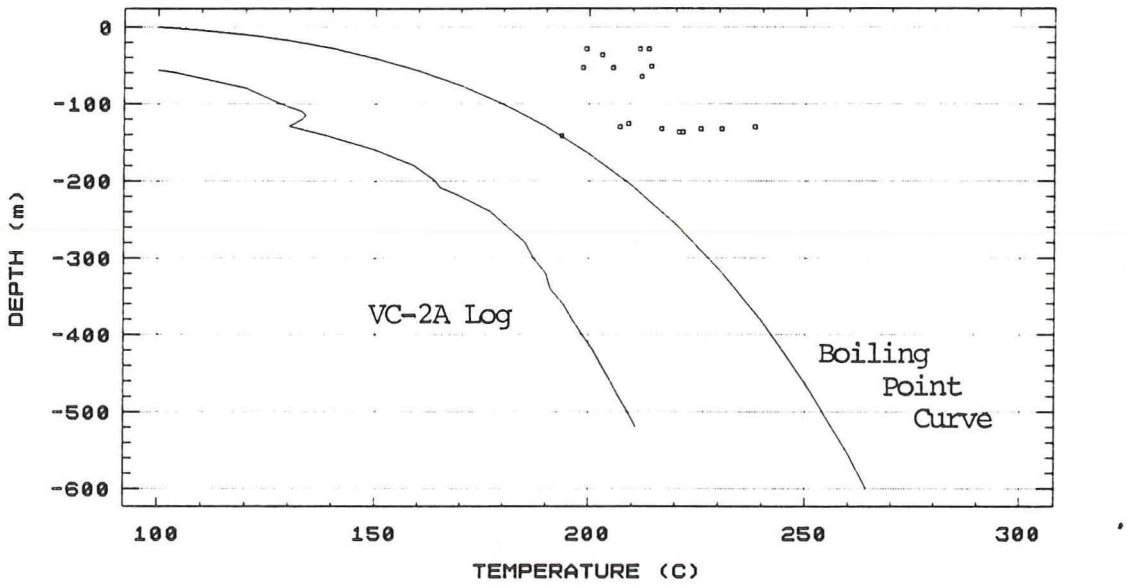

Figure 11B

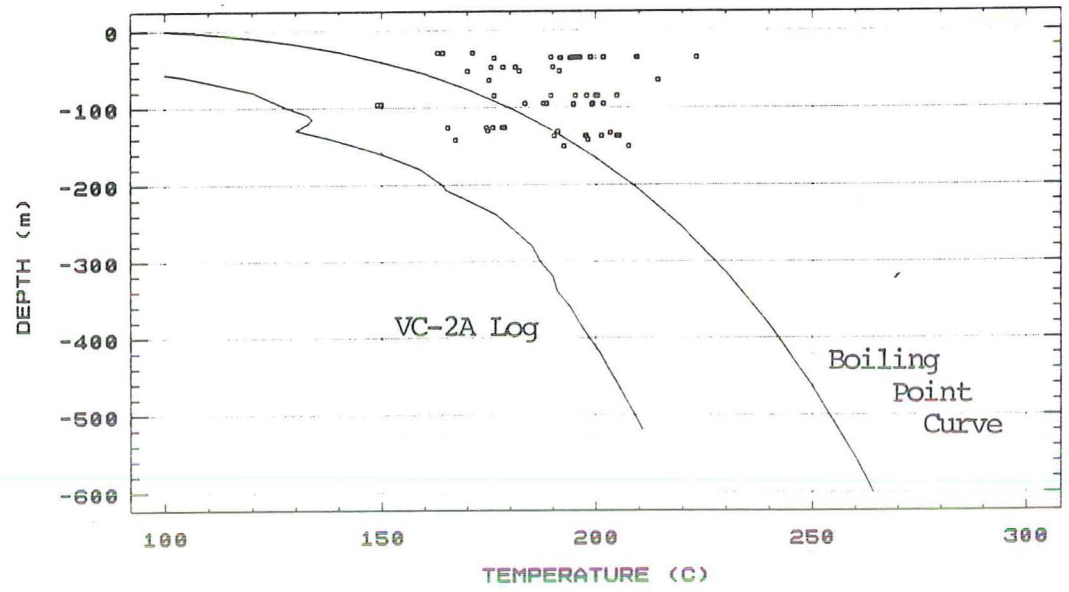

Figure 12A: Homogenization temperature of primary inclusions in fluorite.

Figure 12B: Homogenization temperature of secondary inclusions in fluorite.

Figure 12A

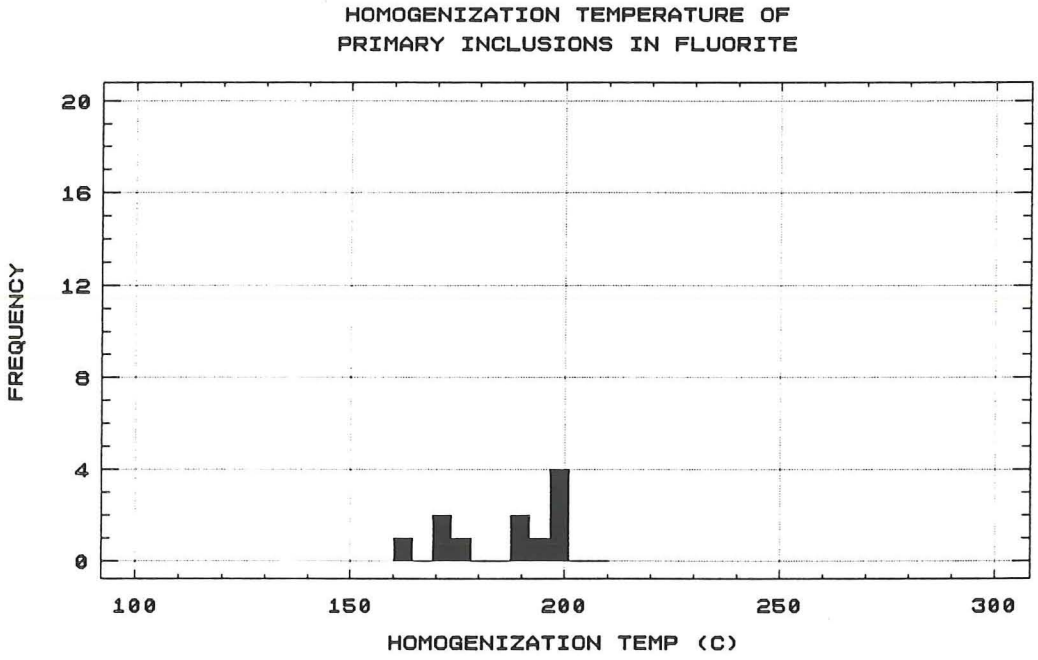

Figure 12B

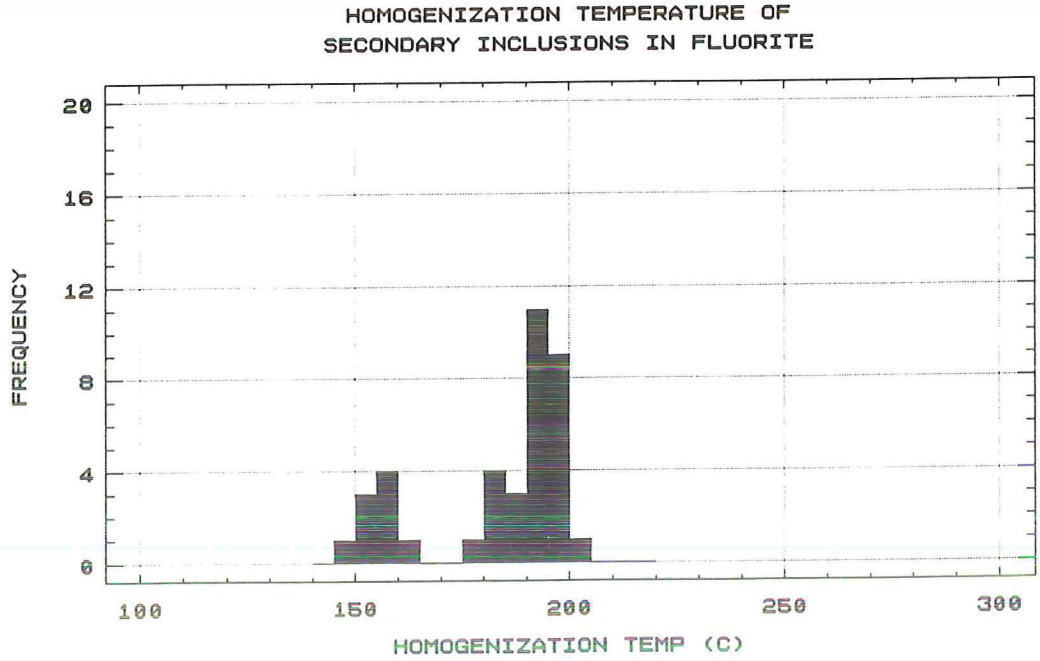

Figure 12C: Homogenization temperature vs. depth for primary inclusions in fluorite.

Figure 12D: Homogenization temperature vs. depth for secondary inclusions in fluorite.

Figure 12C

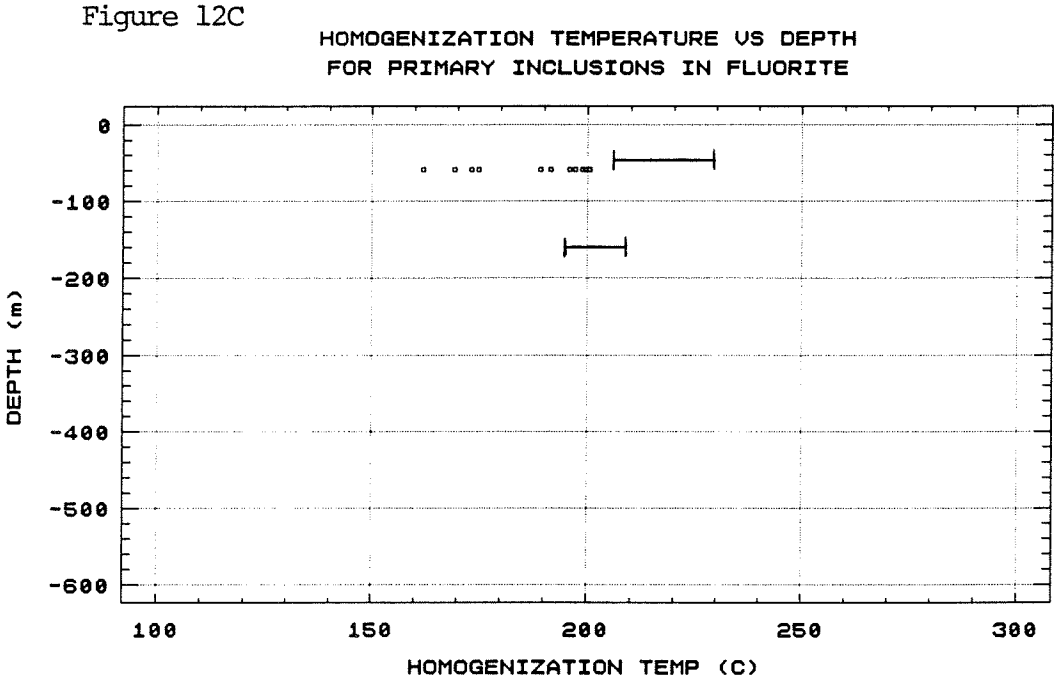

Figure 12D

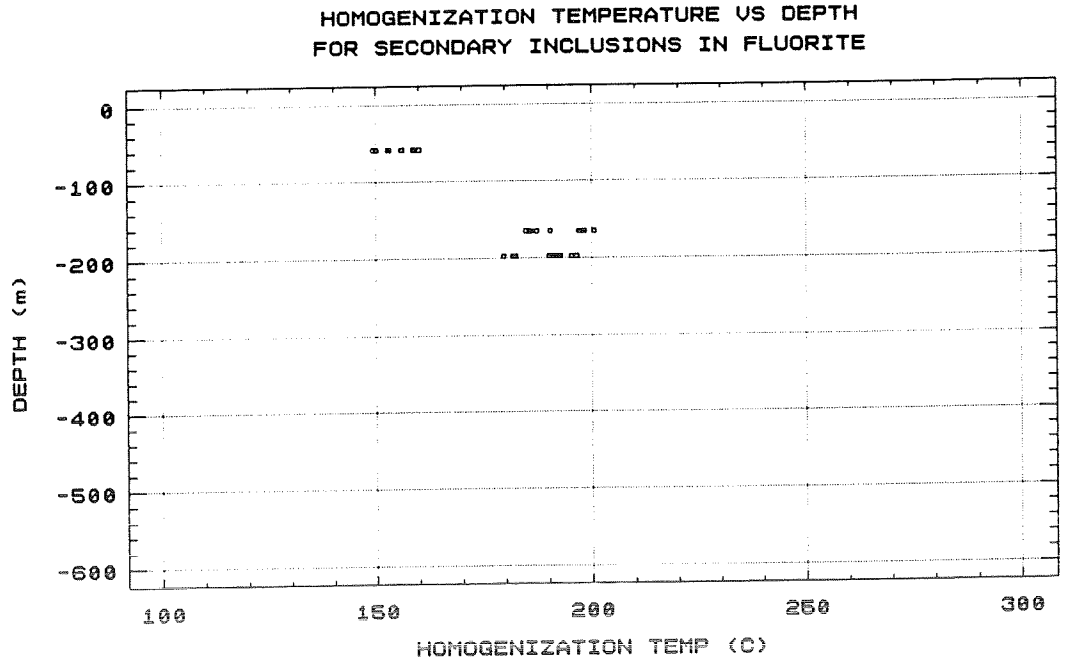

the present study generally range from 150°C to 205°C (Figures 12B, 12D) and seem to increase with depth. However, there are few data points. These temperatures are considerably greater than the downhole temperature log of the well (Figure 13A, 13B). Figures 13A and 13B show that primary inclusions in fluorite homogenized at temperatures greater than the boiling point curve whereas secondaries homogenized at temperatures less than the boiling point curve.

Calcite

Most of the vein calcite could not be studied because the samples were opaque. One sample, the deepest (522m), is a wide vein deposit and, with polishing, was somewhat more useable. The homogenization temperature of the primary inclusion was 309.1°C. Homogenization temperatures of secondary inclusions ranged from 224.7°C to 274.6°C (Figure 9B). Some of these values may be in error since most of the inclusions studied were large and irregular and may have resulted from necking. Small

Figure 13A: VC-2A downhole temperature log with Th of primary inclusions in fluorite, together with the boiling curve for pure water (Haas, 1971).

Figure 13B: VC-2A downhole temperature log with Th of secondary inclusions in fluorite.

Figure 13A

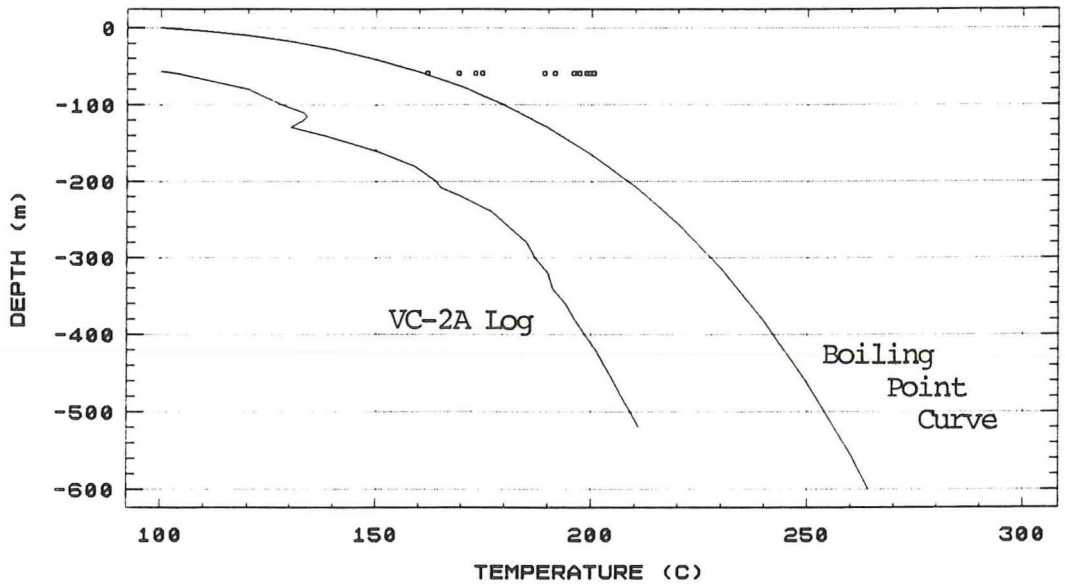

Figure 13B

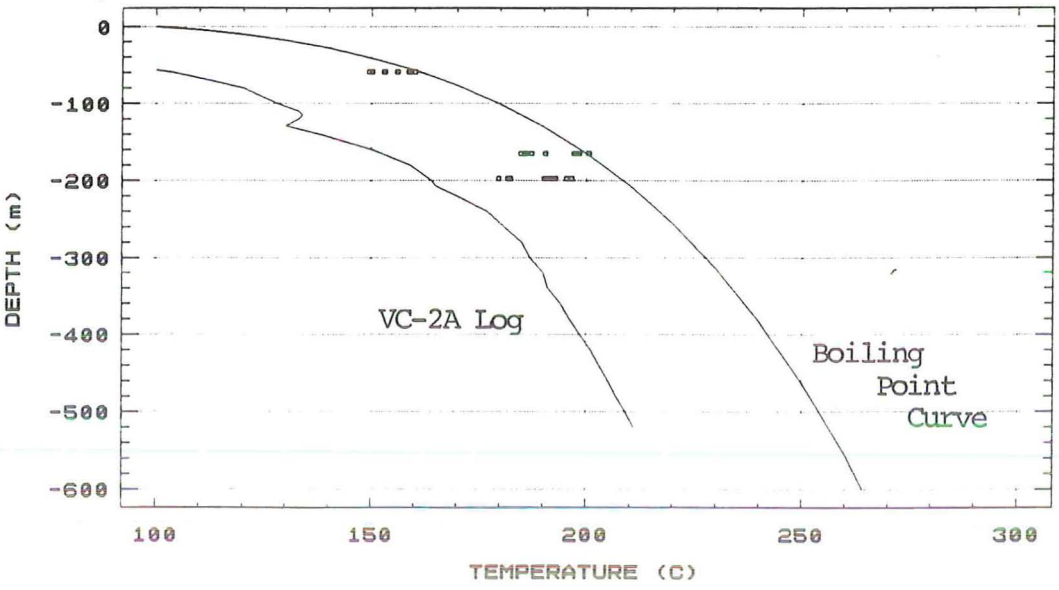

inclusions were difficult to study due to the poor clarity of the crystals. Figure 14 shows that all secondary inclusions homogenized at temperatures greater than the downhole temperature log but that two homogenized at temperatures greater than the boiling point curve.

Crushing

Vapor bubbles of some inclusions in quartz and fluorite expanded during crushing and then dissolved slowly in the immersion oil medium. In the $BaCl_2$ solution, the vapor bubbles in some inclusions would expand and dissolve quickly. In both media, other vapor bubbles did not expand and only slowly contracted.

Figure 14: VC-2A downhole temperature log with Th of secondary inclusions in calcite, together with the boiling curve for pure water (Haas, 1971).

Figure 14

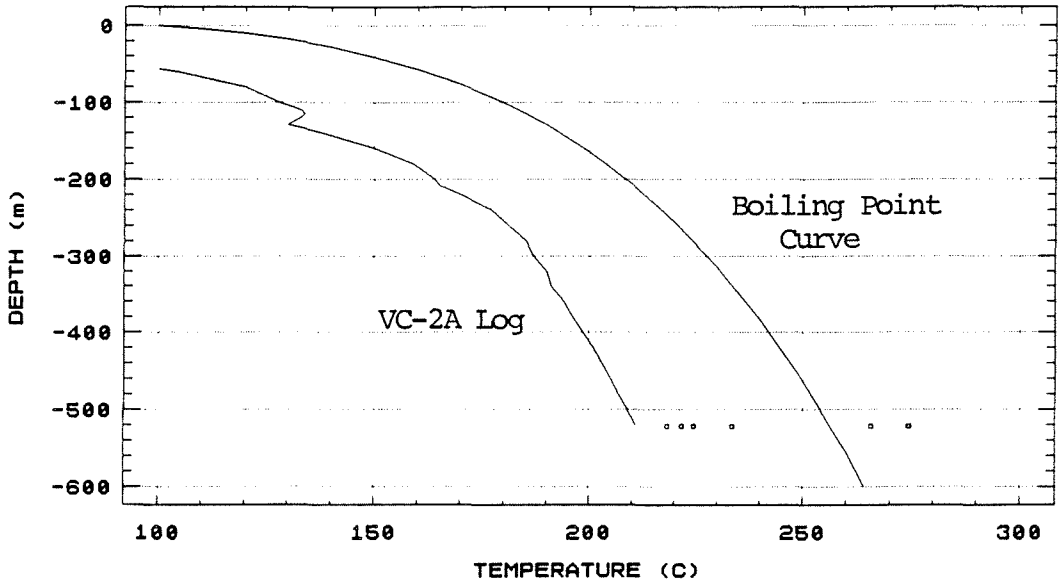
0
-100
-200
-300
-400
-500
-600
DEPTH (m)
100
150
200
250
300
TEMPERATURE (C)
Boiling Point
Curve
VC-2A Log

INTERPRETATION

Freezing

Ice melting temperatures of primary and secondary inclusions in both quartz and fluorite (0.0°C to -0.3°C) indicate that the mineralizing fluid had a very low salinity of approximately 0.0 to 0.53 wt % NaCl equivalents. The overlapping clusters of Tmi values of primary and secondary inclusions suggest that the salinity of the mineralizing fluid has not changed appreciably through time. Also, as can be seen in Figures 7C, 7D, 8C, and 8D, the salinity of the mineralizing fluid is constant with depth indicating that mixing of fluids with different compositions has not occurred over the relatively narrow (150 m) depth range.

The Tmi of primary and secondary inclusions in calcite (0.0°C to -1.0°C) indicates that mineralizing fluids at 522 m were more saline than those which deposited quartz and fluorite higher in the section (1.73 wt. % NaCl vs. 0.53 wt % NaCl).

Heating

Quartz

The measurements of homogenization temperature of primary inclusions in quartz were approximately 213°C. Secondary inclusions in quartz homogenized at approximately 190°C. Figures 10C and 10D show that these temperatures were relatively constant with depth. This suggests that mixing of fluids with greatly differing temperatures either did not occur over this narrow depth range or was masked by the thermal inertia of the host rocks. In comparing primary temperatures with secondary temperatures, it is evident that somewhat cooler ($23\pm$°C) fluids were trapped in later (secondary) inclusions. Further evidence of continued cooling is shown in Figures 11A and 11B in which all the Th values are greater than the downhole temperature log (November 1986) and all primaries and some of the secondaries homogenized at temperatures greater than the boiling point curve. Therefore, a history of cooling since mineralization is evident.

The larger range (75°C vs 45°C) in homogenization temperature values of secondary inclusions (150°C to 225°C), as opposed to primaries (195°C to 240°C), in the quartz might be explained by a drop in temperature of the system, so that secondary inclusions trap cooler fluid through time. Ranges in Th could also occur if the fluid was boiling at the time of trapping. However, this can not be verified because homogenization temperatures of the few vapor-rich inclusions were not measurable. However, Sasada (1988) states that boiling was occuring during deposition (Hulen et.al., 1988).

Homogenization temperatures of primary inclusions in this study (213°C) indicate that the hydrostatic head at the depth where trapping occurred would be at least 200 m as constrained by the boiling point curve for pure water (Figure 11A, 11B) (Haas, 1971). This is in agreement with the findings of Goff et al. (1987b) that the liquid phase must have extended approximately 200 m above the present ground surface.

Fluorite

Both primary and secondary homogenization temperatures in fluorite suggest a bimodal distribution (two groupings) of data points (Figures 12A, 12B). This may indicate two different episodes of fluorite mineralization. The first episode may be recorded by the relatively higher temperature primaries (Th=189°C to 205°C) and secondaries (Th=180°C to 205°C), while the lower sets of primaries at Th=160°C to 178°C and secondaries of Th=147°C to 163°C may represents a second episode. If a cooling trend is assumed, the Th of the higher- temperature group of primary inclusions would indicate that this fluorite was deposited later than the quartz, and the lower- temperature fluorite even later. Hulen et al. (1987) report fluorite homogenization temperatures that are higher than those in quartz which may be indicative of a higher temperature episode of fluorite mineralization that was not sampled by this study. Hulen (personal communication, 1988) indicated that the fluorite sampled during his study was an early, minor pre-quartz fluorite

and that most fluorite in VC-2A is of later mineralization.

Calcite

The high homogenization temperature of primary (309.1°C) and secondary (224.7°C to 274.6°C) inclusions in calcite, as well as the greater salinity, indicate that the calcite was deposited from mineralizing fluids different from those higher in the section. The differences may be a result of cooling and dilution by meteoric waters as the fluids ascended since some calcite is present in very small veins within the tightly sealed rock. Another explanation is that since the calcite sample was separated from the other vein deposits by approximately 322 m of tightly sealed rock, upward movement of the hotter, more saline fluid was constrained and did not significantly contribute to the fluids higher in the section. In either case, the constraining rocks may have increased the pressure from hydrostatic to partial lithostatic. Hydrostatic pressure from the surface to approximately 200 m would have been about 1.96 MPa; lithostatic pressure for the region from 200

m to 522 m would have been about 8.37 MPa (assuming density of the rock to be 2.65 kg/m^3). The temperature correction for 10.33 MPa of pressure for Th of 309.1°C would be approximately 10°C (assuming 1% NaCl) (Potter, 1977). Therefore, primary inclusions in calcite were trapped at approximately 320°C.

Crushing

Since CO_2 is the major non-condensible gas in most geothermal fields (Hedenquist and Henly, 1985), it is likely that CO_2 is present in these inclusions. The crushing studies indicated that some inclusions contained a non-condensable gas since the vapor bubbles expanded upon release. This gas is most likely CO_2 since the expanded vapor bubbles collapsed slowly in immersion oil and rapidly in $BaCl_2$. The expansion of the vapor bubbles with no other evidence of CO_2 (e.g. clathrate or liquid CO_2 detectable during freezing) indicates that 0.01 to 0.9 mol % CO_2 may be

present (Sasada, 1985). In some inclusions in which the vapor bubbles did not expand, a non-condensable gas was not present as the vapor pressure was less than or equal to one atmosphere. The absence or presence of CO_2 in inclusions within the same crystal may be due to changes in CO_2 composition in the mineralizing fluids during history of crystal growth and secondary healing. If the fluid was boiling, degassing could also explain the lack of CO_2 in some inclusions.

Because CO_2 depresses the melting temperature of ice, an apparent increase in the inferred total salinity results in low-NaCl fluids (Hedenquist and Henley, 1985). Therefore, the presence of CO_2 in the fluids requires that the reported NaCl equivalent salinity be taken as a maximum value rather than as an absolute.

CONCLUSIONS

A low salinity (<0.53 wt % NaCl eq.), low temperature (213°C) fluid was responsible for the formation of quartz and fluorite veins originally deposited at hydrostatic pressures corresponding to depths approximately 175m greater than present depth. Salinity has not significantly varied since that time and CO_2 is probably present in some inclusions in quantities less than 0.9 mol %.

Primary inclusions in quartz were trapped at temperatures approximately 23°C higher than the temperatures at which secondary inclusions were trapped. This difference plus the wide range of secondary inclusion homogenization temperatures seems to represent a relatively continuous trapping of cooling fluids down to 150°C. Minimum homogenization temperatures of primary and secondary inclusions are 20°C to 50°C higher than the present downhole temperature of the well. These observations indicate that the Valles caldera geothermal fluids below Sulphur

Springs have been progressively cooling since mineralization.

Hulen et al. (1987) report homogenization temperatures in fluorite that are higher than those in quartz, which suggest that some fluorite was deposited prior to quartz. However, the results of this study indicate two episodes of fluorite mineralization, both at temperatures less than that of primary inclusions in quartz, indicating that the fluorite was deposited subsequent to the quartz. It is most likely that the results of Hulen et al. (1987) are representative of an episode of fluorite mineralization which preceeded quartz mineralization and which was not sampled by this study.

The calcite appears to have been deposited from fluids of low salinity (1.73 wt. % NaCl) at a temperature of approximately 320°C under partial lithostatic pressure. Both the salinity and trapping temperature are higher than for inclusions in the quartz and fluorite. This may have resulted because the calcite depositing fluids were isolated from the large fractures higher in the section by the tightly sealed rocks. It is also possible that the

calcite mineralizing fluid did reach the higher fractures, as evidenced by very small calcite veins in the tightly sealed rocks, but were cooled and diluted by meteoric waters prior to quartz and fluorite mineralization.

The results of this study support the findings of Goff et al. (1987) in that the depth of trapping of inclusions in quartz and fluorite was approximately 200 m or 175 m greater than the present depth. This depth can be accounted for by a now-drained caldera lake or a now-eroded host rock which had fractures open to the surface.

Necking of inclusions may have masked any original evidence of trapping of boiling fluids in the system; the few solitary vapor-rich inclusions observed may represent the remnants of such evidence. If boiling or effervescence occurred during this mineralization, it could also explain some of the range in Th values, differences in CO_2 content, and may have been the

driving force behind the deposition of the molybdenite by the coupled reactions:

$$H^+ + HCO_3^- \rightarrow CO_{2(g)} + H_2O$$

$$Mo^{2+} + 2H_2S + 0.5O_2 \rightarrow MoS_2 + 2H^+ + H_2O.$$

REFERENCES

Bailey, R.A., and Smith, R.L., 1978, Volcanic geology of the Jemez Mountains, New Mexico; in Hawlely, J.W., ed., Guidebook to the Rio Grande rift in New Mexico and Colorado; New Mexico Bur. Mines Miner. Resour., Circ. 163, p.184-196.

Bayhurst, G.K., and Janeky, D.R., 1987, Investigation of alteration mineralogy and geochemistry in CSDP hole VC-2A, Valles caldera, New Mexico, (abs.); Eos, v. 68, n. 16, p. 469.

Charles, R.W., Buden, R.J.V., and Goff, F., 1986, An interpretation of the alteration assemblages at Sulphur Springs, Valles caldera, New Mexico; Jour. Geophys. Res., v. 91, n. B2, p. 1887-1898.

Dondanville, R.F., 1978, Geologic characteristics of the Valles caldera geothermal system, New Mexico; Transactions of Geothermal Resources Council, v. 2, p. 157-160.

Goff, F.E. and Bolivar, S.L., 1983, Field trip guide to the Valles Caldera and its geothermal systems; Los Alamos National Laboratory, LA-9963-OBES, UC-66a, 53p.

Goff, F., Gardner, J.N., Grigsby, C.O., Maassen, L., and Shevenell, L., 1985a, The thermal regime of CSDP corehole VC-1, Valles Caldera, New Mexico, (abs.); Eos, v. 66, n. 46, p. 1080.

Goff, F., Gardner, J.N., Shevenell, L., Rowley, J., 1987a, Preliminary results of CSDP core hole VC-2A, Sulphur Springs, Valles caldera, New Mexico, (abs.); Eos, v. 68, n. 16, p. 469.

Goff, F., Gardner, J.N., Vidale, R., and Charles, R., 1985b, Geochemistry and isotopes of fluids from Suphur Springs, Valles caldera, New Mexico; Jour. of Volcanology and Geothermal Research, v. 23, p. 273-297.

Goff, F. and Grigsby, C.O., 1982, Valles caldera geothermal systems, New Mexico, U.S.A.; Jour. of Hydrology, v. 56, p. 119-136.

Goff, F.E., Grigsby, C.O., Trujillo, P.E., Jr., Counce, D., and Kron, A., 1981, Geology, water geochemistry and geothermal potential of the Jemez Springs area, Canon de San Diego, New Mexico; Jour. of Volcanology and Geothermal Research, v. 10, p. 227-244.

Goff, F., Nielson, D.L., Gardner, J.N., Hulen, J.B., Lysne, P., Shevenell, L., and Rowley, J.C., 1987b, Scientific drilling at Sulphur Springs, Valles caldera, New Mexico: Core hole VC 2A; Eos, v. 68, n. 30, p. 649, 661-662.

Goff, F., Rowley, J., Gardner, J.N., Hawkins, W., Goff, S., Charles, R., Wachs, D., Maassen, L., and Heiken, G., 1986, Initial results from VC-1, first scientific drilling program, core hole in Valles Caldera, New Mexico; Jour. Geophys. Resear., v. 91, n. B2, p. 1742-1752.

Goff, F., Rowley, J., Gardner, J.N., Hawkins, W., Goff, S., Pisto, L., and Polk, G., 1985c, History and results of VC-1, the first CSDP corehole in Valles caldera, New Mexico; Trans. Geotherm. Resour. Counc., v. 9, p. 435-440.

Haas, J.L., Jr., 1971, The effect of salinity on the maximum thermal gradient of a hydrothermal system at hydrostatic pressure; Economic Geology, v. 66, p. 940-946.

Hedenquist, J.W., and Henley, R.W., 1985, The importance of CO_2 on freezing point measurements of fluid inclusions: Evidence from active geothermal systems and implications for epithermal ore deposition; Economic Geology, v. 80, p. 1379-1406.

Hulen, J.B., Nielson, D.L., Goff, F., Gardner, J.N., and Charles, R.W., 1987, Molybdenum mineralization in an active geothermal system, Valles caldera, New Mexico; Geology, v. 15, p. 748-752.

Hulen, J.B., Gardner, J.N., Nielson, D.L., and Goff, F., 1988, Stratigraphy, structure, hydrothermal alteration and ore mineralization encountered in CSDP corehole VC-2A, Sulphur Springs area, Valles caldera, New Mexico: A detailed overview; Univ. of Utah Res. Inst., Earth Sci. Lab. Rept. ESL-88001-TR, for U.S. Dept. of Energy, Office of Basic Energy Sci., Agreement No. DE-FG02-86ER13555, 44p.

Janecky, D.R., Charles, R., and Goff, F., 1987, Geochemistry of molybdenum bearing assemblages in CSDP well VC-2A, Valles caldera, New Mexico; Eos, v. 68, n. 16, p. 469-470.

Musgrave, J.A., Goff, F., Shevenell, L., Trujillo, P.E., Jr., Counce, D., Luedemann, G., Garcia, S., Dennis, B., Hulen, J., Janik, C., Tomei, F.A., 1989, Selected data from continental scientific drilling core holes VC-1 and VC-2a, Valles Caldera, New Mexico; Los Alamos National Laboratory, LA-11496-OBES, UC-403, 71 p.

Nielson, D.L., Goff, F., 1985, Scientific drilling in a vapor-dominated geothermal system, VC-2A, Sulphur Springs, Valles caldera, New Mexico, (abs.); Eos, v. 66, n. 46, p. 1082.

Potter, R.W., II, 1977, Pressure corrections for fluid-inclusion homogenization temperatures based on the volumetric properties of the system NaCl-H_2O; U.S. Geological Survey Journal of Research, v. 5, p. 603-605.

Roedder, E., 1984, Fluid Inclusions; in Ribbe, P.H., ed., Reviews in Mineralogy; Mineralogical Society of America, v. 12, 644p.

Sasada, M., 1985, CO_2-bearing fluid inclusions from geothermal fields; Geothermal Resources Council Transactions, v. 9, part 1, p. 351-356.

Sasada, M., 1988, Microthermometry of fluid inclusions from the VC-1 core hole in Valles Caldera, New Mexico; Jour. Geophys. Resear., v. 93, n. B6, p. 6091-6096.

Smith, R.L., and Bailey, R.A., 1967, Stratigraphy, structure, and volcanic evolution of the Jemez Mountains, New Mexico, (abs.); Geol. Soc. Amer. Spec. Papers, n. 115, p. 447-448.

Smith, R. L., and Bailey, R.A., 1968, Resurgent cauldrons, in Coats, R.R., Hay, R.L., and Anderson, C.A., Studies in volcanology; Geol. Soc. Amer., Mermoir 116, p. 613-662.

Smith, S.P., and Kennedy, B.M., 1985, Noble gas evidence for two fluids in the Baca (Valles caldera) geothermal reservoir; Geochim. Cosmochim. Acta, v. 491, p. 893-903.

Starquist, V.L., 1988, Core log Valles caldera #2A, New Mexico; Los Alamos National Laboratory, LA-11176-OBES, UC-66B.

Truesdell, A.H., and Janik, C.J., 1986, Reservoir processes and fluid origins in the Baca geothermal system, Valles caldera, New Mexico, Jour. Geophys. Resear., v. 91, n. B2, p. 1817-1833.

Vuataz, F.D., and Goff, F., 1986, Isotope geochemistry of thermal and nonthermal waters in the Valles Caldera, Jemez Mountains, Northern New Mexico; Jour. Geophys. Resear., v. 91, n. B2, p. 1835-1853.

Westra, G., and Keith, S.B., 1981, Classification and genesis of stockwork molybdenum deposits; Economic Geology, v. 76, p. 844-873.

White, A.F., 1986, Chemical and isotopic characteristics of fluids within the Baca geothermal reservoir, Valles caldera, New Mexico; Jour. Geophys. Resear., v. 91, n. B2, p. 1855-1866.

White, A.F., Delany, J.M., Truesdell, A., Janik, K., Goff, F., and Crecraft, H., 1984, Fluid chemistry of the Baca geothermal field, Valles caldera, New Mexico; Field Conference Guidebook 35, New Mexico Geological Society, p. 257-263.

White, W.H., Bookstrom, A.A., Kamilli, R.J., Ganster, M.W., Smith, R.P., Ranta, D.E., and Steininger, R.C., 1981, Character and origin of climax-type molybdenum deposits; Economic Geology, 75th Anniversary Volume, p. 270-316.

Plate 1: Primary inclusion in fluorite from a depth of 164.6 m. Inclusion is approximately 60 micrometers in length.

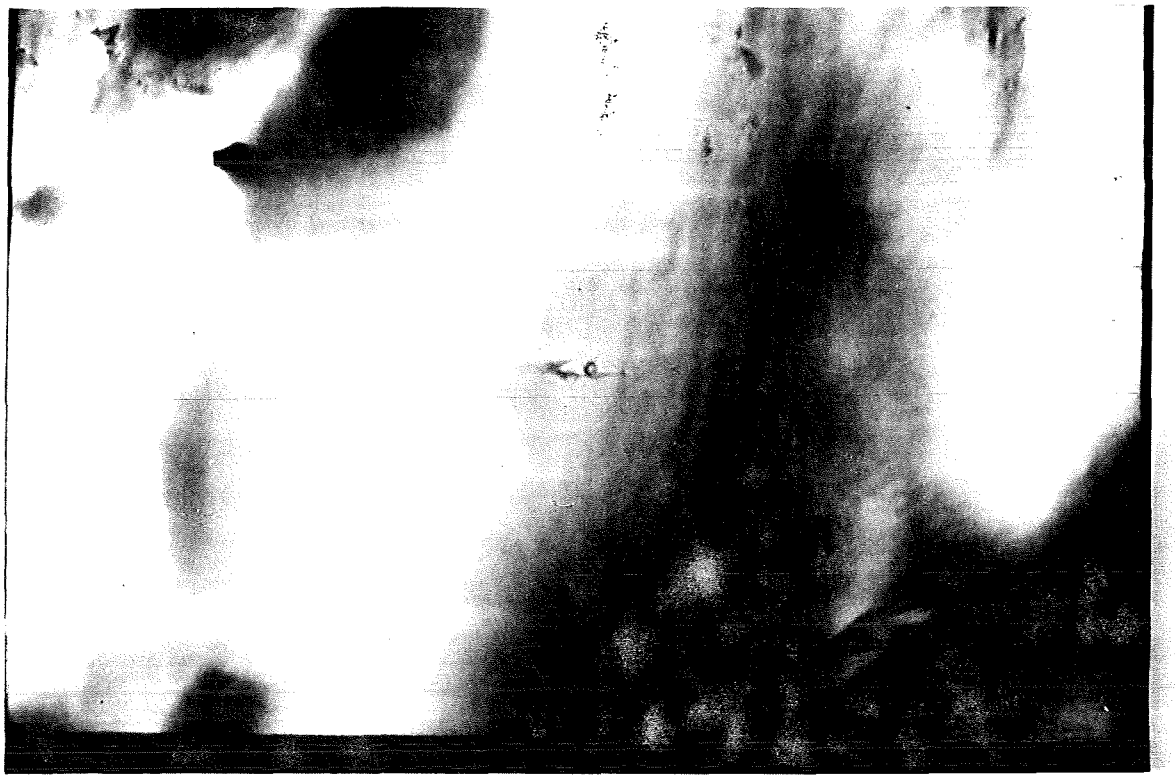

Plate 2: Secondary inclusions in fluorite from a depth of 164.6 m. Inclusions range from 6 to 9 micrometers in length.

Plate 3: Necked inclusions in fluorite from a depth of 164.6 m. Largest inclusion is approximately 18 micrometers in length.

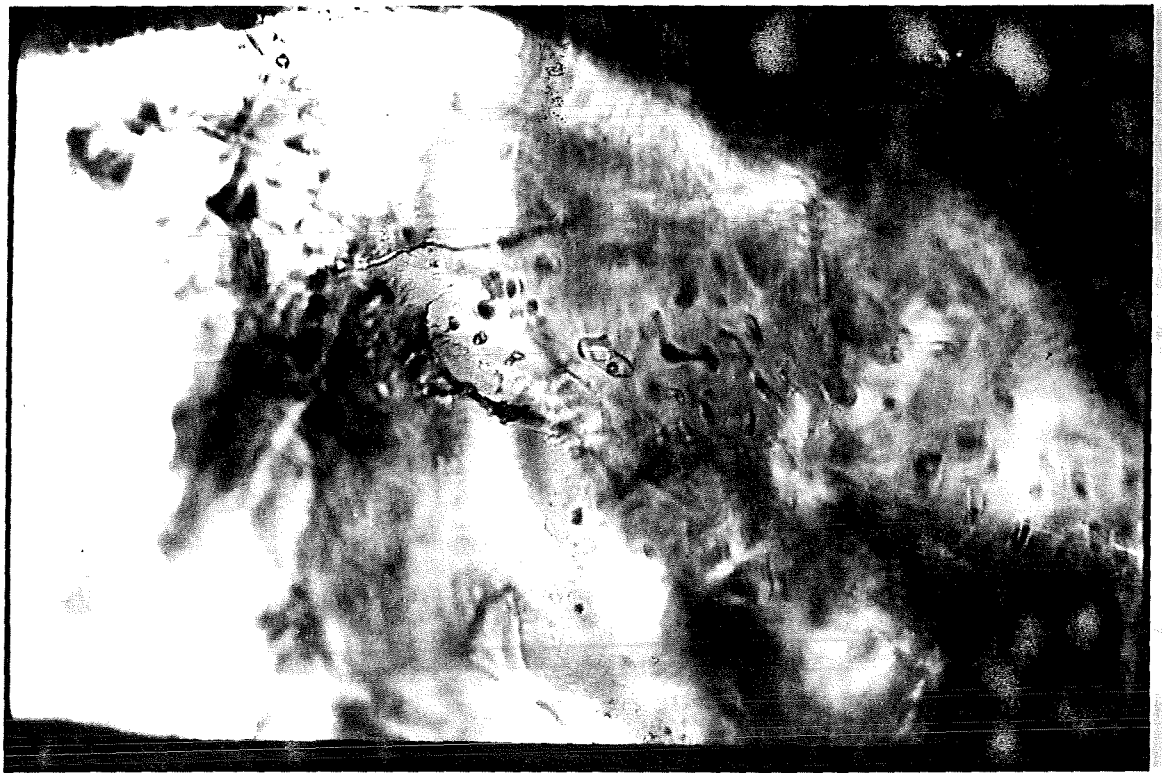

Plate 4: Vapor-rich primary inclusion in quartz from a depth of 47.9m. Inclusion is approximately 45 micrometers in length.

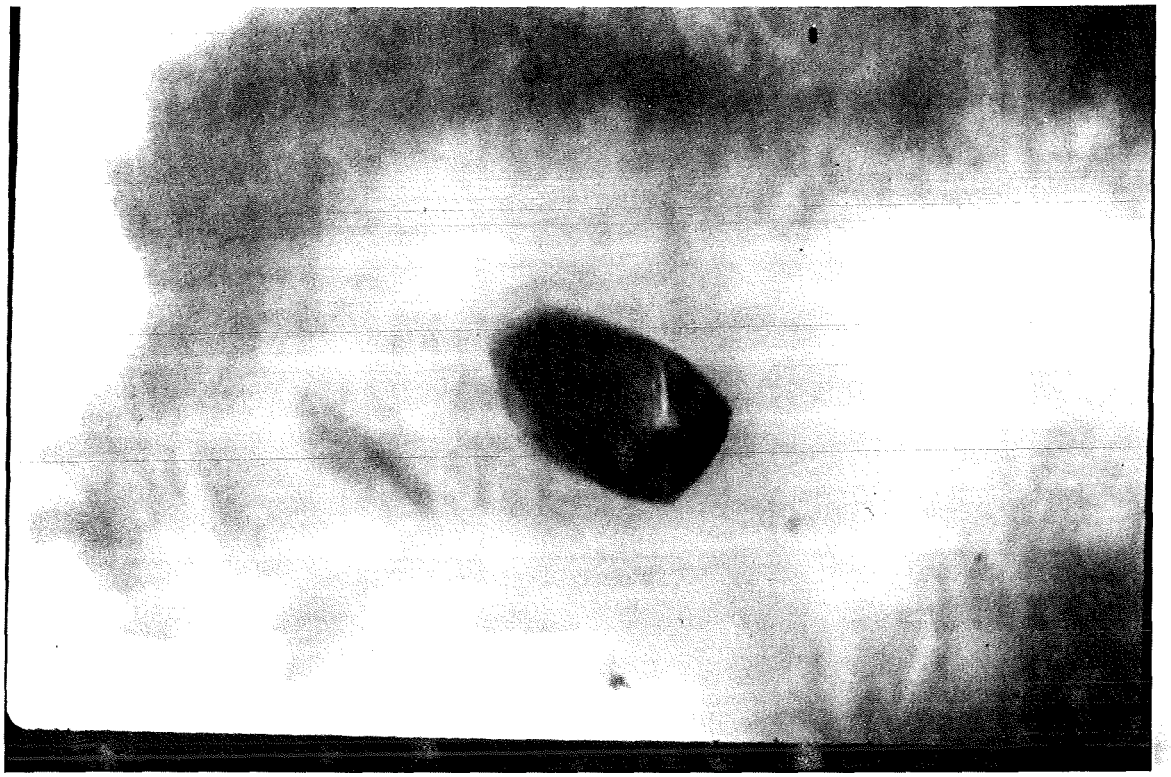

APPENDIX A: Descriptions of Cores Studied

Sample 27-7 Depth 29.0 m

The core consists of white and gray unsorted agglomerate which is moderately indurated with a medium to low porosity and is highly altered. Quartz crystals are subhedral to anhedral and occur with fine grained euhedral crystals of pyrite.

Sample 31-5 Depth 35.1 m

The core is a densely welded lapillie tuff with euhedtral quartz and pyrite crystals grown in vugs. Molybdenite also occurs, altering to ilsemanite. Fractures are subvertical and range from less than 1 mm to 5 mm in width.

Sample 32-7 Depth 36.0 m

The core is a densely welded lapilli tuff with euhedral quartz and pyrite crystals in the fracture vugs. Molybdenite may also be present. Fractures are subvertical and less than 1 mm in width. Vugs are up to 5 mm in width.

Sample 43-1 Depth 47.9 m

The core is a densely welded lapilli tuff with abundant euhedral quartz crystals in the vugs and fine grained euhedral pyrite crystals. Molybdenite may be present. Fractures are subvertical and about 2 mm in width.

Sample 45-3A Depth 51.4 m

The core is a densely welded lapilli tuff with euhedral quartz and pyrite crystals filling the fractures. Molybdenite may be present. Fractures are vertical and range from 1 mm to 3 mm in width while vugs are about 5 mm in width.

Sample 46-3 Depth 52-7 m

The core is a densely welded lapilli tuff with euhedral quartz and pyrite crystals in the fractures. Fractures are subvertical and approximately 4 mm in width.

Sample 50-7 Depth 59.0 m

The core is a densely welded lapilli tuff with euhedral quartz in fractures. Fine grained pyrite also occurs and fluorite and molybdenite may also be present. Fractures are subvertical and range from 1 mm to 3 mm in width.

Sample 68-1 Depth 84.5 m

The core is a densely welded lapilli tuff with euhedral quartz, pyrite, and molybdenite occurring on a fracture surface. Fractures are vetical and about 2 mm in width.

Sample 74-9 Depth 94.5 m

The core is a densely welded lapilli tuff with euhedral quartz and pyrite occurring in fracture veins. Molybdenite may be present. Fractures are vertical and range from 1 mm to 3 mm in width.

Sample 75-2 Depth 95.4 m

The core is a densely welded lapilli tuff with euhedral quartz and pyrite occurring in fracture veins and vugs. Fractures are subvertical and range from 1 mm to 2 mm in width.

Sample 96-7A Depth 126.1 m

The core is a densely welded lapilli tuff with euhedral quartz and pyrite crystals occurring in vugs. Also a white clay is present. Fractures are subvertical and range from 1 mm to 2 cm in width.

Sample 99-1B Depth 129.7 m

The core is a densely welded lapilli tuff with euhedral quartz and pyrite occurring in vugs. Subhedral sphalerite(?) occurs on a fracture surface. Fractures are subvertical and range from 1 mm to 2 mm in width.

Sample 99-7 Depth 131.1 m

The core is a densely welded lapilli tuff with euhedral quartz and pyrite crystals occurring in fractures. One fracture contains two large euhedral quartz crystals (1 cm long, each). White clay is also present. Fractures are subvertical and range from 4 mm to 2 cm in width.

Sample 100-8 Depth 132.2 m

The core is a welded lapilli tuff with a vessicular texture. Vugs contain euhedral quartz, pyrite, and white clay. The core is highly altered. Fractures are subvertical and range from 2 mm to 2 cm in width.

Sample 103-7 Depth 136.4 m

The core is a densely welded lapilli tuff with euhedral quartz and sphalerite(?) occurring on a fracture plane and euhedral pyrite occurring in white clay. Fractures are subvertical and range from 1 mm to 5 mm in width.

Sample 107-1 Depth 141.8 m

The core is a densely welded lapilli tuff with a large vug containing euhedral quartz, white clay, and fine grained pyrite. Fractures are subvertical and range from 1 mm to 1 cm in width.

Sample 113-2 Depth 149.7 m

The core is a densely welded lapilli tuff with euhedral quartz, rhodocrosite, white clay and fine grained pyrite occurring in one large vug. Other smaller vugs contain quartz, pyrite, and clay. Fractures are subvertical and range from 1 mm to 1.5 cm in width.

Sample 122-7 Depth 164.6 m

The core is a highly altered lapilli tuff with one large vein filled with fluorite. Another surface is coated in white clay. Fractures are subvertical and about 1 cm in width.

Sample 145-5 Depth 197.3 m

The core is an extremely altered welded lapilli tuff with white to green clay. Also contains fluorite and calcite. Fractures are subvertical and about 1 cm in width.

Sample 362-3 Depth 522.0 m

The core is a highly altered lapilli tuff with a large calcite vein and green clay. The calcite vein comprises most of the core sample.

APPENDIX B: Fluid Inclusion Data

Sample	Depth(m)	Mineral	Type[1]	Tmi(°C)	Th(°C)
27-7	29.0	Quartz	P	*[2]	211.7
27-7	29.0	Quartz	P	-0.2	199.2
27-7	29.0	Quartz	P	-0.2	213.8
31-5	35.1	Quartz	S	*	105.8
31-5	35.1	Quartz	S	*	194.7
31-5	35.1	Quartz	S	*	209.4
31-5	35.1	Quartz	S	*	209.6
31-5	35.1	Quartz	S	*	198.7
31-5	35.1	Quartz	S	*	223.3
31-5	35.1	Quartz	S	*	194.6
31-5	35.1	Quartz	S	*	201.7
31-5	35.1	Quartz	S	*	196.2
31-5	35.1	Quartz	S	*	189.5
32-7	36.0	Quartz	S	0.0	194.0
32-7	36.0	Quartz	S	0.0	191.7
32-7	36.0	Quartz	S	-0.1	176.3
32-7	36.0	Quartz	P	-0.2	203.0
32-7	36.0	Quartz	S	-0.2	191.6

[1]Type: P = Primary Inclusion, S = Secondary Inclusion

[2]Tmi(°C): * = no data

Sample	Depth(m)	Mineral	Type	Tmi(°C)	Th(°C)
43-1	47.9	Quartz	S	-0.1	178.3
43-1	47.9	Quartz	S	-0.1	181.2
43-1	47.9	Quartz	S	*	175.5
43-1	47.9	Quartz	S	*	190.0
43-1	47.9	Quartz	S	*	190.0
45-3A	51.4	Quartz	P	*	214.4
46-3	52.7	Quartz	S	0.0	191.5
46-3	52.7	Quartz	S	0.0	170.0
46-3	52.7	Quartz	S	0.0	182.0
46-3	52.7	Quartz	P	*	198.5
46-3	52.7	Quartz	P	*	205.4
50-7	59.0	Fluorite	S	-0.2	153.1
50-7	59.0	Fluorite	S	-0.1	160.2
50-7	59.0	Fluorite	P	-0.1	198.7
50-7	59.0	Fluorite	S	-0.1	158.6
50-7	59.0	Fluorite	S	-0.2	158.2
50-7	59.0	Fluorite	S	*	149.4
50-7	59.0	Fluorite	S	-0.3	159.0
50-7	59.0	Fluorite	P	-0.2	195.8
50-7	59.0	Fluorite	P	-0.1	197.1
50-7	59.0	Fluorite	S	-0.2	156.2
50-7	59.0	Fluorite	S	*	156.0

Sample	Depth(m)	Mineral	Type	Tmi(°C)	Th(°C)
50-7	59.0	Fluorite	P	0.0	174.7
50-7	59.0	Fluorite	P	0.0	169.2
50-7	59.0	Fluorite	P	0.0	162.0
50-7	59.0	Fluorite	P	0.0	173.1
50-7	59.0	Fluorite	S	*	150.2
50-7	59.0	Fluorite	P	-0.2	200.4
50-7	59.0	Fluorite	P	-0.2	189.1
50-7	59.0	Fluorite	P	-0.1	191.4
50-7	59.0	Fluorite	P	-0.2	199.5
54-7	64.9	Quartz	S	*	175.0
68-1	84.5	Quartz	S	0.0	176.2
68-1	84.5	Quartz	S	0.0	199.9
68-1	84.5	Quartz	S	0.0	200.4
68-1	84.5	Quartz	S	*	197.9
68-1	84.5	Quartz	S	0.0	204.8
74-9	94.5	Quartz	S	-0.3	188.4
74-9	94.5	Quartz	S	-0.3	187.7
74-9	94.5	Quartz	S	-0.3	183.4
74-9	94.5	Quartz	S	-0.3	201.7
75-2	95.4	Quartz	S	-0.1	194.8
75-2	95.4	Quartz	S	*	149.8
75-2	95.4	Quartz	S	-0.2	199.1
75-2	95.4	Quartz	S	*	149.0

Sample	Depth(m)	Mineral	Type	Tmi(°C)	Th(°C)
96-7A	126.1	Quartz	P	0.0	209.0
96-7A	126.1	Quartz	S	-0.1	176.0
96-7A	126.1	Quartz	S	-0.1	165.3
96-7A	126.1	Quartz	S	0.0	174.5
96-7A	126.1	Quartz	S	-0.2	178.6
96-7A	126.1	Quartz	S	-0.2	178.2
99-1B	129.7	Quartz	S	-0.2	147.8
99-1B	129.7	Quartz	P	-0.2	238.3
99-1B	129.7	Quartz	P	-0.2	207.1
99-7	131.1	Quartz	S	*	191.2
100-8	132.2	Quartz	P	-0.2	230.6
100-8	132.2	Quartz	P	-0.2	216.8
100-8	132.2	Quartz	S	-0.3	203.4
100-8	132.2	Quartz	P	-0.2	225.9
103-7	136.4	Quartz	S	-0.3	201.3
103-7	136.4	Quartz	S	-0.2	205.3
103-7	136.4	Quartz	S	-0.2	204.9
103-7	136.4	Quartz	S	-0.2	197.5
103-7	136.4	Quartz	S	*	197.7
103-7	136.4	Quartz	S	-0.2	190.2
103-7	136.4	Quartz	P	-0.2	220.8
103-7	136.4	Quartz	P	-0.3	221.7
107-1	141.8	Quartz	S	0.0	198.2

Sample	Depth(m)	Mineral	Type	Tmi(°C)	Th(°C)
113-2	149.7	Quartz	S	*	192.5
113-2	149.7	Quartz	S	*	207.6
122-7	164.6	Fluorite	S	-0.3	190.4
122-7	164.6	Fluorite	S	-0.2	184.8
122-7	164.6	Fluorite	S	-0.3	185.9
122-7	164.6	Fluorite	S	-0.2	187.3
122-7	164.6	Fluorite	S	-0.2	184.7
122-7	164.6	Fluorite	S	-0.2	185.7
122-7	164.6	Fluorite	S	-0.2	198.3
122-7	164.6	Fluorite	S	-0.2	197.6
122-7	164.6	Fluorite	S	0.0	197.9
122-7	164.6	Fluorite	S	0.0	197.4
122-7	164.6	Fluorite	S	0.0	197.5
122-7	164.6	Fluorite	S	-0.2	198.1
122-7	164.6	Fluorite	S	-0.1	200.5
122-7	164.6	Fluorite	S	-0.2	196.9
145-5	197.3	Fluorite	S	-0.2	190.1
145-5	197.3	Fluorite	S	-0.1	191.5
145-5	197.3	Fluorite	S	-0.1	192.4
145-5	197.3	Fluorite	S	-0.2	192.8
145-5	197.3	Fluorite	S	-0.2	190.7
145-5	197.3	Fluorite	S	-0.2	190.8
145-5	197.3	Fluorite	S	-0.3	190.6

Sample	Depth(m)	Mineral	Type	Tmi(°C)	Th(°C)
145-5	197.3	Fluorite	S	-0.2	192.7
145-5	197.3	Fluorite	S	0.0	196.5
145-5	197.3	Fluorite	S	0.0	179.6
145-5	197.3	Fluorite	S	-0.1	181.7
145-5	197.3	Fluorite	S	-0.1	182.3
362-3	522.0	Calcite	S	-0.4	221.9
362-3	522.0	Calcite	S	-0.6	218.4
362-3	522.0	Calcite	S	-0.1	224.7
362-3	522.0	Calcite	P	-0.5	309.1
362-3	522.0	Calcite	S	-1.0	274.3
362-3	522.0	Calcite	S	-1.0	274.6
362-3	522.0	Calcite	S	-0.1	233.7
362-3	522.0	Calcite	S	0.0	265.8